INL/EXT-16-38431
Revision 0

AGC-2 Irradiation Report

David Rohrbaugh
William Windes
W. David Swank

June 2016

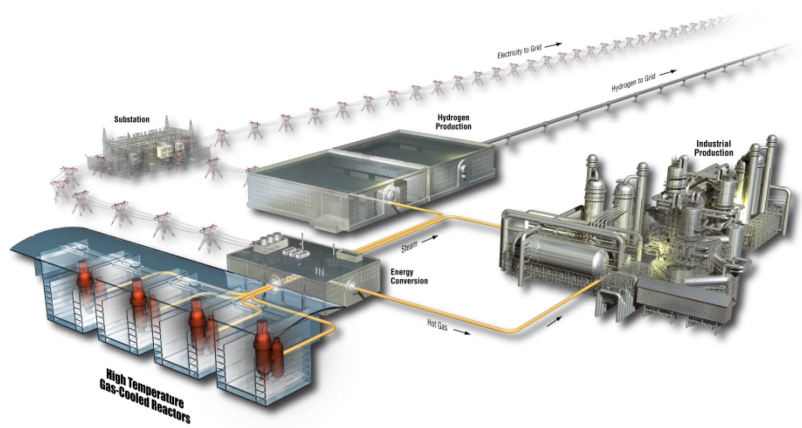

The INL is a
U.S. Department of Energy
National Laboratory
operated by
Battelle Energy Alliance

Idaho National Laboratory

INL/EXT-16-38431
Revision 0

AGC-2 Irradiation Report

David Rohrbaugh
William Windes
W. David Swank

June 2016

Idaho National Laboratory
INL ART TDO Program
Idaho Falls, Idaho 83415

http://www.inl.gov

Prepared for the
U.S. Department of Energy
Office of Nuclear Energy
Under DOE Idaho Operations Office
Contract DE-AC07-05ID14517

INL ART TDO Program

AGC-2 Irradiation Report

INL/EXT-16-38431
Revision 0

June 2016

Author:

6/17/2016
Date

David Rohrbaugh
INL ART Graphite Researcher

Technical Reviewer: (Confirmation of mathematical accuracy, correctness of data, and appropriateness of assumptions.)

6/17/2016
Date

William Windes
INL ART Graphite R&D Program Technical Lead

Approved by:

6/17/16
Date

Diane Croson
INL ART TDO Deputy Director

6/20/16
Date

Michael Davenport
INL ART Project Manager

6/17/16
Date

Michelle T. Sharp
INL ART TDO Quality Assurance

SUMMARY

The Advanced Graphite Creep (AGC)-2 capsule is the second of six planned irradiation capsules comprising the AGC experiment test series. During the AGC experiment, graphite specimens are irradiated and stressed for comparison to irradiated unstressed and unirradiated specimens to garner the quantitative data necessary for predicting the irradiation behavior and operating performance of new nuclear-grade graphite. This testing will ascertain the in-service behavior of the graphite for pebble-bed and prismatic very high-temperature reactor designs. Similar to the first AGC (i.e., AGC-1) pre-irradiation examination report, material property tests were conducted on specimens from 16 nuclear-grade graphite types. However, AGC-2 tested an increased number of specimens (i.e., 486) compared to AGC-1 (i.e., 366) [1]. The AGC-2 capsule was irradiated in the Advanced Test Reactor at Idaho National Laboratory at approximately 600°C and to a peak dose of 5.0 displacements per atom. All of the irradiated specimen measurements for AGC-2 were conducted at Idaho National Laboratory from April 2014 to March 2015.

This report describes the requirements and design of the second AGC (i.e., AGC-2) irradiation capsule. It summarizes how corrections were made to the specimen elevation due to thermal expansion, irradiation shrinkage, and creep. This correction allows a more accurate prediction of each specimen's temperature and dose. It also details how an average temperature, dose, and load is derived from the capsule thermocouple temperatures, reactor flux profile, and load cell data is summarized, along with a brief discussion about the uncertainty in these values. Tables containing specimen dose, temperature, and load are included in the appendices of this document for use in future creep analysis and material properties comparisons.

CONTENTS

FIGURES

TABLES

ABBREVIATIONS AND ACRONYMS

AGC	advanced graphite creep
ATR	Advanced Test Reactor
dpa	displacements per atom
ECAR	engineering calculation and analysis report
INL	Idaho National Laboratory
MCNP	Monte Carlo N-Particle Transport Code
HTGR	High Temperature Gas-Cooled Reactors

AGC-2 Irradiation Report

1. PROGRAM OVERVIEW

The High Temperature Gas-Cooled Reactors (HTGR) will be helium-cooled, very high-temperature reactor with a large graphite core. In past applications, graphite has been used effectively as a structural and moderator material in both research and commercial high-temperature gas-cooled reactor designs [2][3]. Nuclear graphite H-451 that was previously in the United States for nuclear reactor graphite components is no longer available. New nuclear graphites have been developed and are considered suitable candidates for the new NGNP reactor design. To support the design and licensing of NGNP core components within a commercial reactor, a complete properties database must be developed for these current grades of graphite. Quantitative data on in-service material performance are required for the physical, mechanical, and thermal properties of each graphite grade, with a specific emphasis on data related to the life-limiting effects of irradiation creep on key physical properties of the NGNP candidate graphite.

Based on experience with previous graphite-core components, the phenomenon of irradiation-induced creep within the graphite has been shown to be critical to the total useful lifetime of graphite components. Irradiation-induced creep occurs under the simultaneous application of high temperatures, neutron irradiation, and applied stresses within the graphite components. Significant internal stresses within the graphite components can result from a second phenomenon (i.e., irradiation-induced dimensional change). In this case, the graphite physically changes (i.e., first shrinking and then expanding with increasing neutron dose). This disparity in material-volume change can induce significant internal stresses within graphite components. Irradiation-induced creep relaxes these large internal stresses, thus reducing the risk of crack formation and component failure. Obviously, higher irradiation-creep levels tend to relieve more internal stress, thus allowing the components longer useful lifetimes within the core. Determining the irradiation-creep rates of nuclear-grade graphite is critical for determining the useful lifetime of graphite components and is a major component of the Advanced Graphite Creep (AGC) experiment.

The AGC test series is comprised of six individual capsules, each containing over 350 graphite specimens that will be irradiated in one of the large flux traps of the Advanced Test Reactor (ATR) at Idaho National Laboratory (INL) [4]. As a whole, this experimental series will examine the properties and behavior of nuclear-grade graphite over a large spectrum of temperatures, irradiation fluencies, and applied stress that are expected to induce irradiation creep strains within a very high-temperature reactor graphite component. The AGC series is currently underway; the irradiated specimen measurements for AGC-2 were conducted from April 2014 to March 2015. This characterization will be used to determine the in-service behavior of new graphite for both pebble-bed and prismatic reactor designs. Further details about research and development activities and associated rationale required to qualify nuclear-grade graphite for use within the NGNP are documented in the NGNP graphite technology research and development plan [4][5].

2. EXPERIMENT DESIGN REQUIREMENTS

The following requirements for graphite specimens were identified (these conditions, along with the requirements for the facility, system, and engineering design, can be found in TFR-645, "Advanced Graphite Capsule AGC-2 experiment test train") [6]:

1. All graphite specimens shall be fresh and unirradiated during initial experiment fabrication.
2. The graphite specimens and their relative position within the test train shall be as specified by the NGNP graphite material properties technical lead and DWG-600786 [7], ATR advanced graphite capsule (AGC-2) graphite specimen machining details.

3. Specimen minimum fast neutron fluence (E>0.1 MeV) > 0.5 × 1021 n/cm^2.
4. Specimen maximum fast neutron fluence (E>0.1 MeV) < 8.5 × 1021 n/cm^2.
5. Reasonable efforts shall be taken in the design of the test train materials and dimensions to limit the fast fluence difference between graphite specimens at equal axial locations above and below the core centerline to not more than 10%.
6. The specimen stacks will have the capability of being placed under a maximum 3,000 psi axial compressive stress on a nominal half inch diameter specimen. The loads placed on the stacks will be evenly distributed diametrically to prevent a shift in the test internals and a change in the gas flow clearances.
7. The specimen volume-average temperatures of each large graphite specimen over the irradiation time will be 600 ± 50°C. Best efforts shall be made to attain 600 ± 50°C volume average temperatures over the irradiation time in the small piggy-back specimens as well; however, due to their location within the test train, the temperatures in these specimens may lie outside of this tolerance band.
8. Each large graphite specimen's time average maximum temperature will not be greater than 650°C and each large graphite specimen's time average minimum temperature will not be less than 550°C. Best efforts shall be made to attain 600 ± 50°C time average maximum temperatures over the irradiation time in the small piggy-back specimens as well; however, due to their location within the test train, the temperatures in these specimens may lie outside of this tolerance band.
9. The AGC-2 experiment shall maximize the number of specimens at the required temperature of 600°C along the 4-foot height of the core.

3. EXPERIMENT DESIGN DESCRIPTION

AGC-2 was designed to irradiate various grades of graphite specimens at a temperature of 600°C and to a peak dose of 5.0 dpa. The graphite specimens were irradiated in an instrumented leadout experiment in the south flux trap of ATR. The experiment has an overall length of 350 in. (Figure 1), with the specimen portion comprising 46 in. and being located within the 48-in. fuel region of ATR. Although a 48-in. specimen section was desired, 46 in. was the maximum length shippable in the GE-2000 cask insert. The test train pressure boundary is constructed of 304L stainless steel. The specimen section of the shell has a nominal outside diameter of 2.5 in. with a 0.185 wall thickness. Standoff nubs are incorporated into the wall to allow concentric placement in the reactor flux trap, which ensures there is radially uniform axial coolant flow. Specimens are arranged in seven stacks (Figure 2), with each 0.5-in. diameter stack being placed within an NBG-25 graphite specimen holder.

Sixteen different grades of graphite specimens were arranged into seven stacks. Specimen Stacks 1 through 6 were split horizontally into compressed and uncompressed sections. The compressed stacks were located above the reactor mid-plane, while the uncompressed specimens were located below the reactor mid-plane. The upper sections were loaded via six pneumatic rams that are located above the specimen stacks. These rams provided nominal loads of 400 lb_f to Stack 1 and Stack 4, 500 lb_f to Stack 2 and Stack 5, and 600 lb_f to Stack 3 and Stack 6. The compressed specimen stacks were loaded via a graphite pushrod that transferred the load from the rams to the uppermost specimens. These pushrods were instrumented to record pushrod displacement occurring during the course of irradiation (Figure 3).

Each compressed stack (i.e., upper housing) consisted of eighteen 1-in. long creep specimens, two or four flux monitor holders, and zero or two 0.25-in. long piggyback specimens [8]. Similar to the compressed specimen section, the uncompressed specimen stacks (i.e., lower housing) consisted of eighteen 1-in. long creep specimens, one or three flux monitor holders, and 14 or 16 piggyback specimens. The center stack consisted of 170 uncompressed 0.25-in. long piggyback specimens only and did not incorporate flux monitor holders. Table 1 shows distribution of creep and piggyback specimens across each grade. Table 2 shows the type of specimens in each of the lower and upper housings, along with the number of flux monitors in each stack.

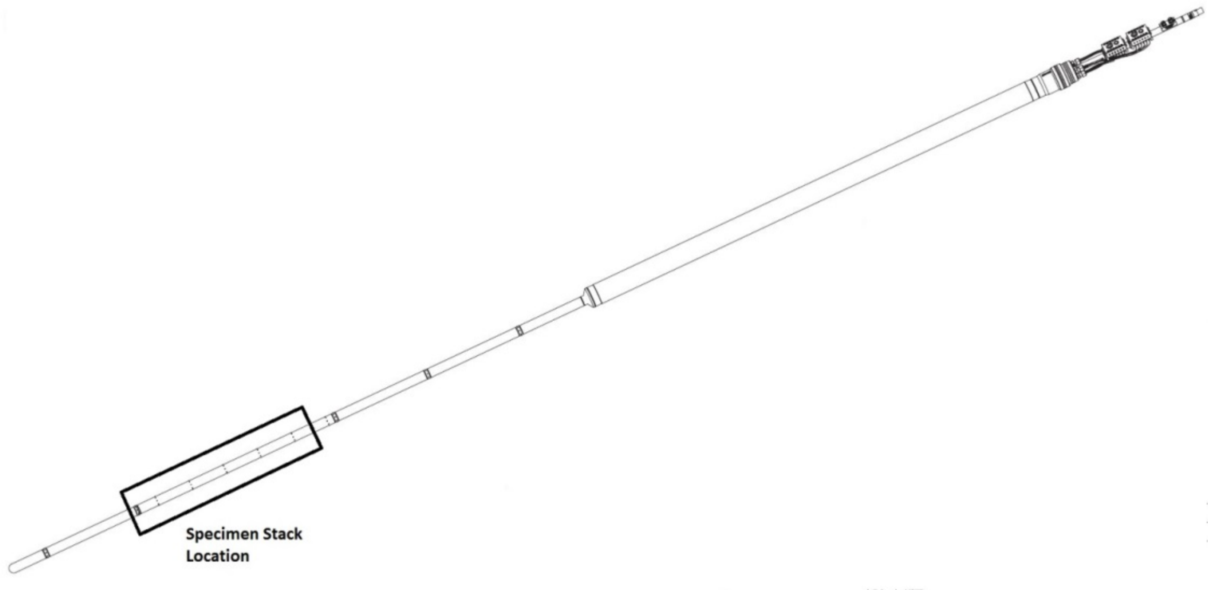

Figure 1. Overall AGC-2 test train arrangement [9].

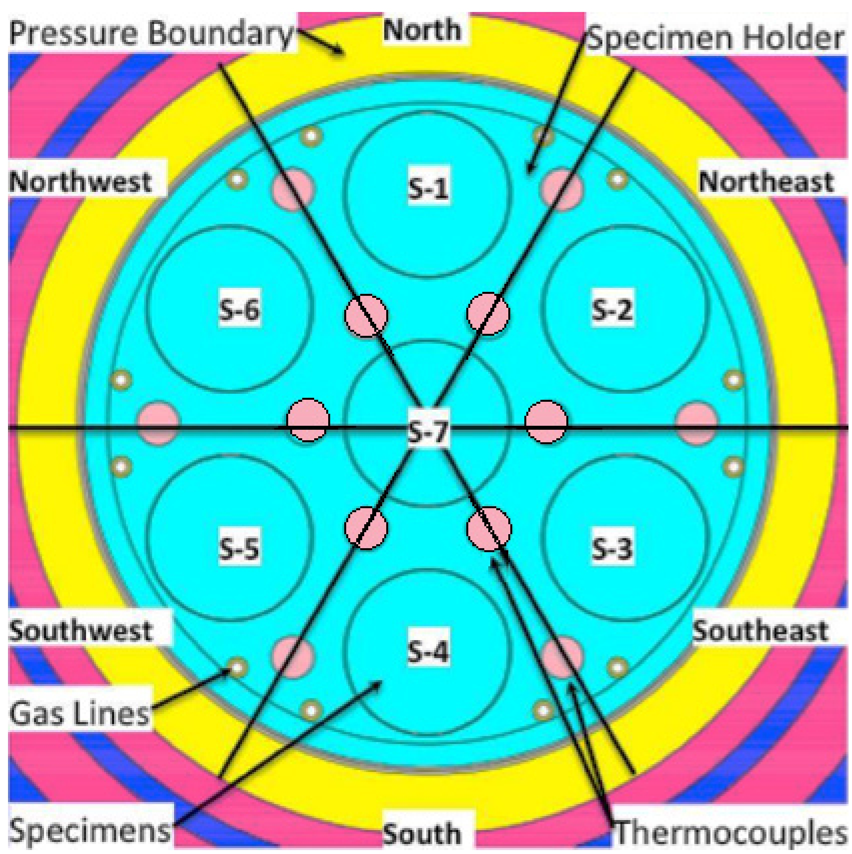

Figure 2. Specimen stack cross section.

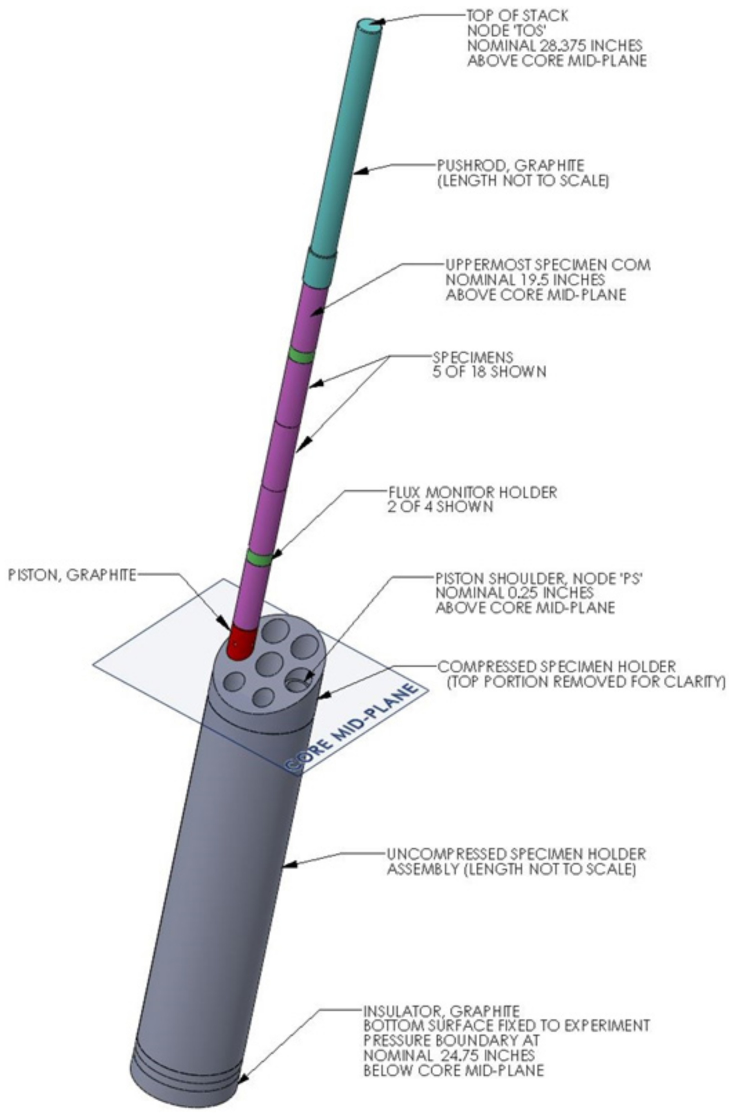

Figure 3. Compressed specimens and graphite specimen holder arrangement.

Table 1. AGC-2 piggyback and creep specimens by grade.

Grade	Stressed Creep	Unstressed Control	Piggyback	Total
2114	0	0	27	27
A3-3 and A3-27	0	0	17	17
BAN	0	0	17	17
H-451	12	12	6	30
HLM	0	0	17	17
IG-110	18	18	21	57
IG-430	18	18	13	49
NBG-10	0	0	17	17
NBG-17	12	12	15	39
NBG-18	24	24	13	61
NBG-25	0	0	17	17
PCEA	24	24	15	63
PCIB	0	0	20	20

Table 1. (continued).

Grade	Stressed Creep	Unstressed Control	Piggyback	Total
PGX	0	0	19	19
PPEA	0	0	20	20
HOPG	0	0	16	16
Totals	108	108	270	486

Table 2. Distribution of specimens and flux monitors by stack and housing.

Stack No.	Housing	Creep	Piggyback	Flux Mon
1	lower	18	14	3
1	upper	18	0	4
2	lower	18	16	1
2	upper	18	2	2
3	lower	18	16	1
3	upper	18	2	2
4	lower	18	14	3
4	upper	18	0	4
5	lower	18	16	1
5	upper	18	2	2
6	lower	18	16	1
6	upper	18	2	2
7	center	0	170	0

In addition to the upper load-inducing pneumatic rams for the compressed specimens, lower rams were also used during planned outages to shift the specimens stacks (i.e., compressed and uncompressed) up and down to assure the specimens do not stick in their graphite holders.

Twelve thermocouples were located within the specimen holders to record and help control specimen temperatures. Although the thermocouples did not directly measure the specimen temperature, the high conductivity of the graphite specimens and graphite holders ensured the radial temperature difference was small and could be readily determined in the thermal analysis. Table 3 lists the elevation of the thermocouples with respect to the core mid-plane, and Figure 4 shows their radial location (TC-01 through TC-12).

Table 3. Thermocouple elevations (inches).

Thermocouple Identifier	Elevation from Core Mid-Plane
TC-01	18.00
TC-02	13.00
TC-03	13.00
TC-04	6.00
TC-05	6.00
TC-06	2.00
TC-07	−6.00
TC-08	−6.00
TC-09	−11.25
TC-10	−18.00
TC-11	−18.00
TC-12	−11.25

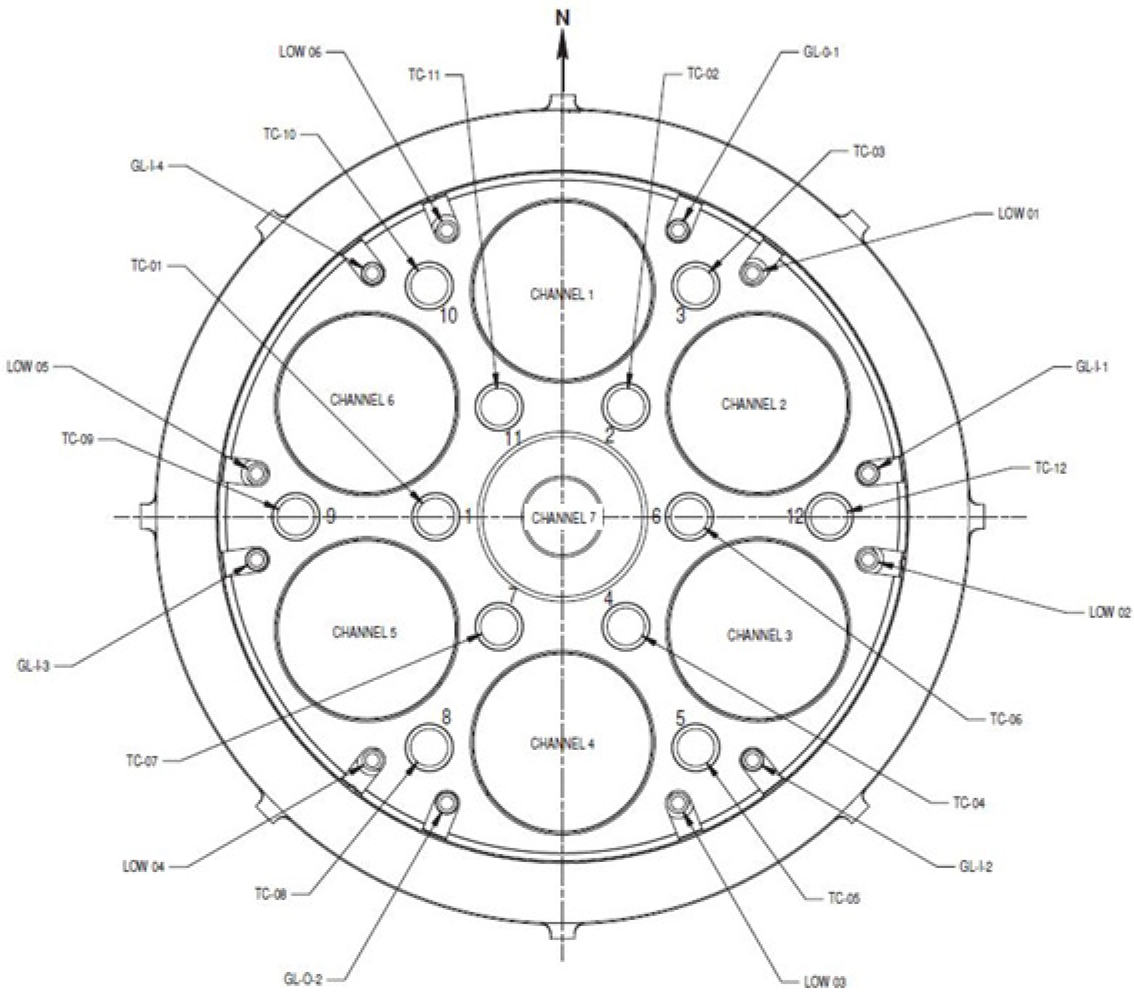

Figure 4. Thermocouple radial location [9].

The temperature within the experiment was controlled by adjusting the mixture of a helium-argon gas stream that affects the conductivity of the gas gap between the specimen holder and the capsule wall. In an effort to maintain a uniform temperature along the axis of the specimen stacks, larger gas gaps were incorporated in the upper and lower sections of the specimen holders that tend to remain cooler due to a decrease in neutron flux. To reduce the radiation heat transfer between the specimen holder and the capsule wall, a 0.002-in. thick stainless steel heat shield was installed between these two surfaces.

The overall design of the AGC-2 capsule was very similar to the AGC-1 design, with the following notable exceptions:

1. The compressed creep specimens and their uncompressed control specimens did not utilize spacers between each specimen.
2. Because spacers were not used, the number of creep specimens in each stack increased from 15 to 18 and the number of control specimens increased from 14 to 18.
3. AGC-2 did not use silicon carbide temperature monitors, which did not require accommodating holes in the piggyback specimens. AGC-2 piggyback specimens did not have center holes machined.
4. The location of the majority of the piggyback specimens in the uncompressed portions of Stacks 1 through 6 changed from the top of the stacks to the bottom of the stacks.

4. EXPERIMENT ASSEMBLY

The experiment was assembled between November 2010 and January 2011 at the Test Train Assembly Facility in the ATR Complex. A critical part of the assembly was loading the specimens into their assigned stacks and in the proper order to ensure the specimens received the desired dose. These assembly instructions and loading order are recorded in ATR Work Order No. 137268 [10]. Because the dose profile varies dramatically as a function of elevation, the loading order (and thus reactor elevational position and capsule axial orientation) was subject to double verification.

5. IRRADIATION HISTORY

The AGC-2 capsule was irradiated between the dates of April 12, 2011, and May 5, 2012 [11]. Figure 5 shows the location of the experiment in the south flux trap of ATR. There were five reactor cycles during this irradiation, Cycles 149A, 149B, 150B, 151A, and 151B (there was no Cycle 150A), for a total of 5,539 megawatt (MW) days or approximately 230 effective full power days. The time history of this irradiation is shown in Figure 6. As can be seen in the figure, there were planned reactor outages between each of the cycles. In addition, there was an unplanned outage in Cycle 151A and two unplanned outages in Cycle 151B.

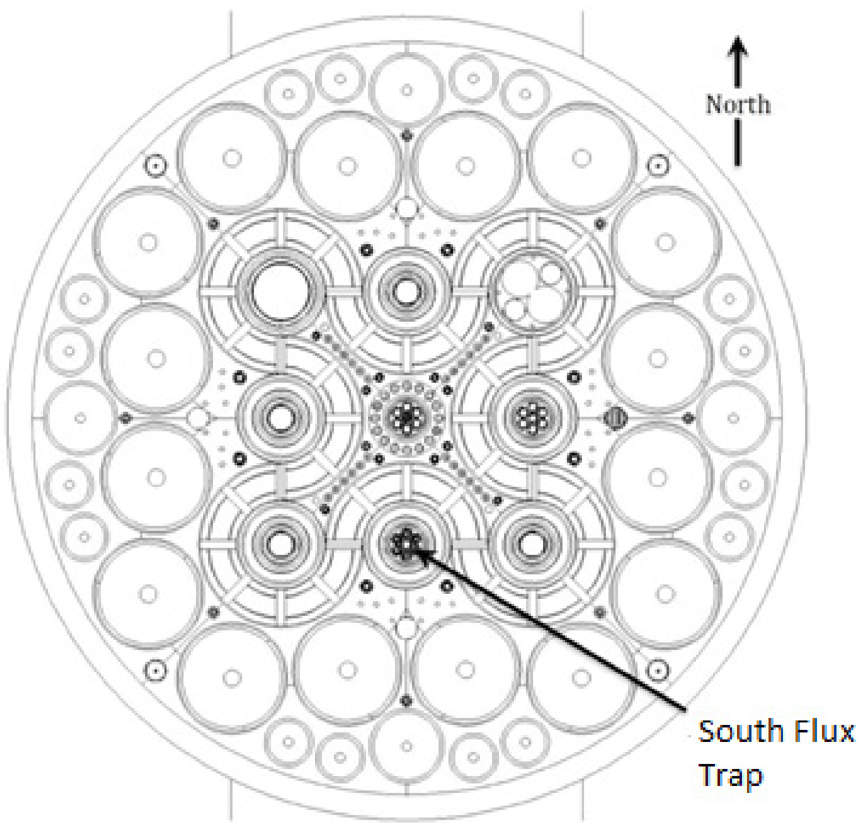

Figure 5. Mid-plane cross section of the ATR core and the location of the south flux trap.

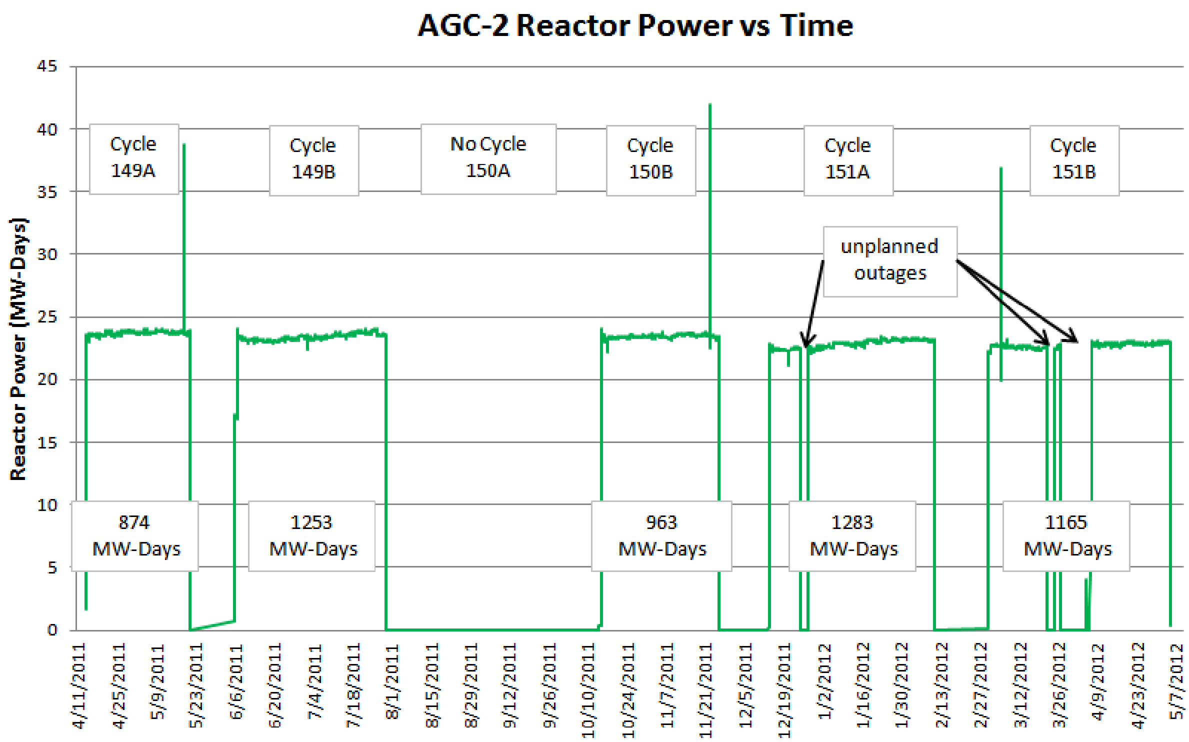

Figure 6. AGC-2 capsule reactor power versus time.

The experiment specimen stacks closest to the reactor centerline received the highest neutron dose. As can be seen in Figure 7, the Cycle 149A dose difference between the stack positions was substantial. In this particular cycle, the north position (i.e., Stack 1) received approximately 25% more dose than the south (i.e., Stack 4) position. To minimize the dose difference between the specimen stacks, the AGC-2 capsule was rotated 180 degrees between Cycles 150B and 151A (about 55% through the total integrated irradiation). As a result, the individual stack doses at a given reactor elevation were equalized (see Figure 8). Thus, the dose difference between Stack 4 and Stack 1 was reduced to 3%. This difference would have been even less if the integrated reactor power before and after the rotation had been equal.

After irradiation, the experiment was removed from the reactor and allowed to cool in the ATR canal. At the end of this decay period, which was necessary to achieve shippable radiation levels, the specimen section of the experiment was cut out of the test train in the ATR dry transfer cell and placed in a shielded cask insert sleeve, which, in turn, was placed in a GE-2000 shipping cask. The specimen stack section was shipped to the Hot Fuel Examination Facility in August 2013 [11]. Disassembly and specimen extraction began February 10, 2014. After the specimens were extracted, they were shipped to the Carbon Characterization Laboratory at the INL Research Center in March 2014 [11]. At the Carbon Characterization Laboratory, specimens were visually inspected, inventoried, and placed into the irradiated graphite storage vault.

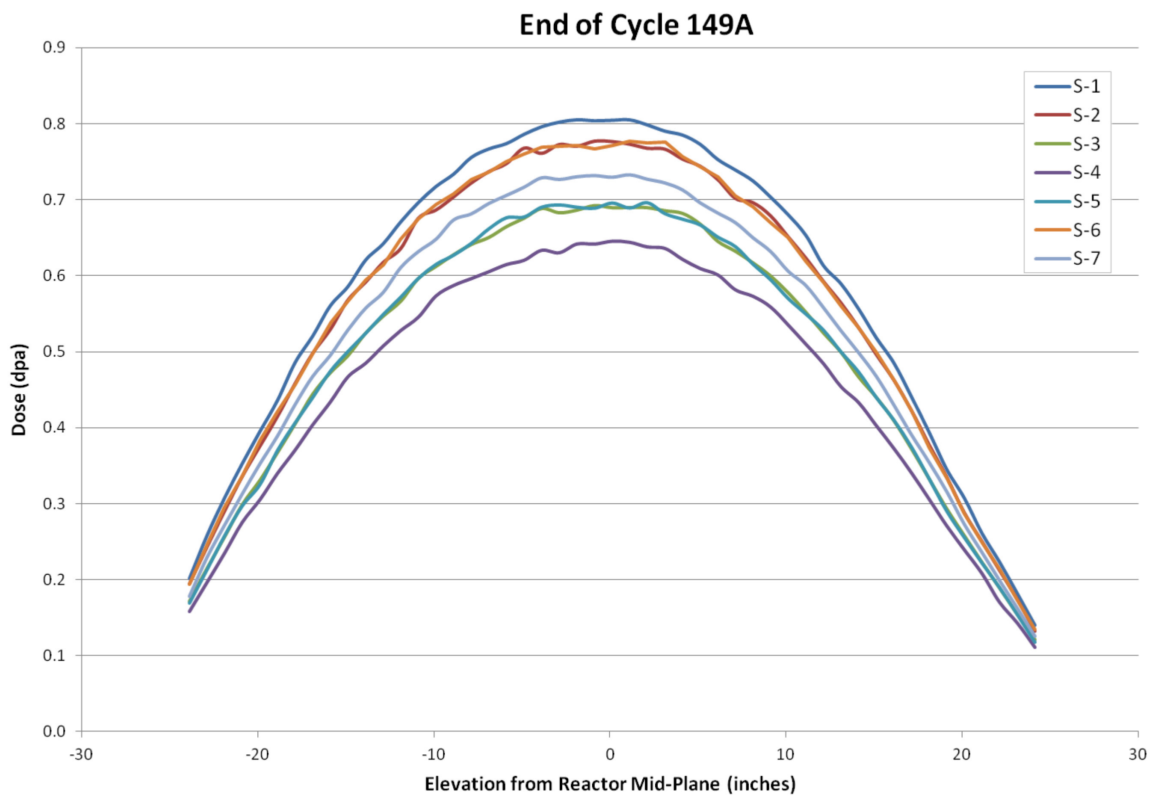

Figure 7. Cycle 149A specimen stack dose comparison.

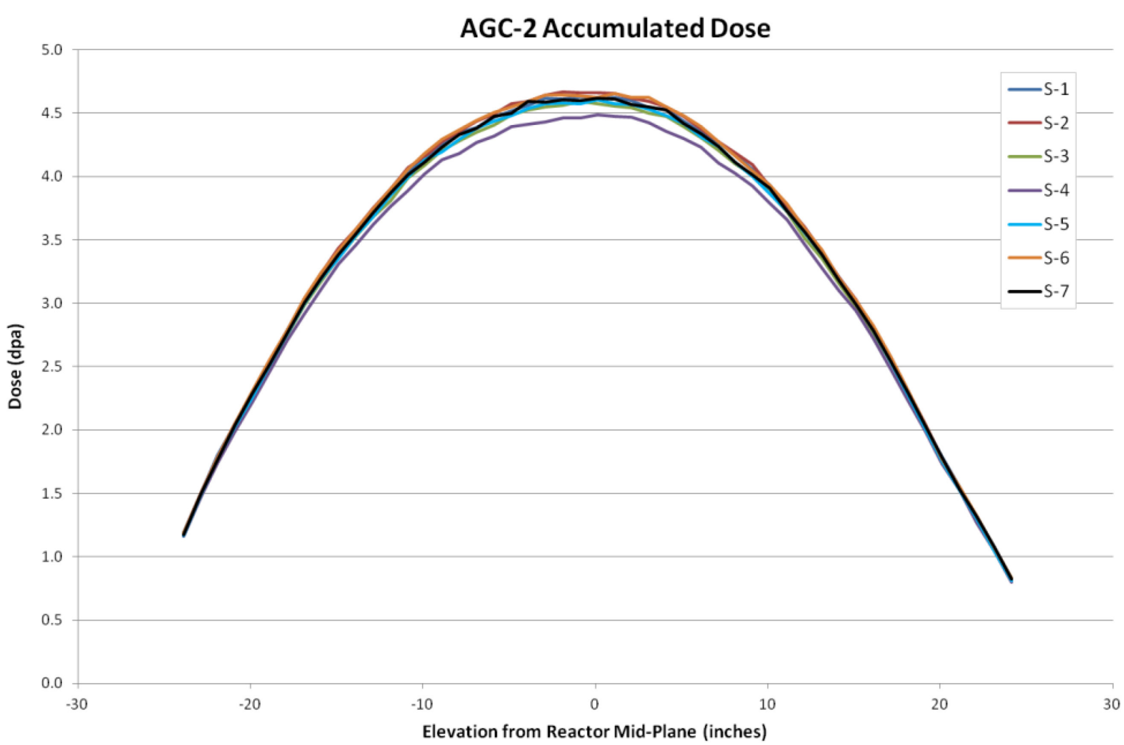

Figure 8. Total accumulated dose of AGC-2 capsule.

6. SPECIMEN ELEVATION ADJUSTMENTS

The dose and temperature of each graphite specimen in the experiment were dependent on its elevation in the reactor and how close they were to the mid-plane of the core. Because of the neutron-induced graphite shrinkage and the creep of the graphite specimens and supporting specimen holders, the uppermost compressed specimens could be displaced as much as 1.4 in. during the irradiation, placing them in an 18% higher dose region. These specimen elevation adjustments were documented in ECAR-2549 [12], where the following influences on specimen position were considered:

1. As-built drawing corrections to the capsules' relative positions in the reactor.

   Prior experiment insertion difficulties have shown that the distance from the reactor top-head closure plate to the core was greater than the nominal elevations shown on the ATR facility drawings. Drawing 600001 lists the measured difference between the closure plate and the gearbox support beam as 0.313 in. greater than the facility drawings. Thus, the height of the specimens in relation to the core mid-plane was 0.313 in. higher than the nominal dimensions. Also, the overall dimension of the experiment was 0.084 in. shorter than the nominal drawing dimension on Drawing 601266. As a further adjustment, the average weld shrinkage of the three capsule welds was 0.035 each, which affected the as-built position of the Lower Isolation Weld Plate (Part No. 601266-9) onto which all graphite components are stacked.

   In addition to the as-built adjustments mentioned above, the specimens also were subject to a stack up error due to their thickness difference from nominal. This effect was most apparent in the center S-7 stack, which had a large number of specimens (i.e., 170 specimens). Per post-irradiation examination measurements, the average S-7 specimen was about 0.0008 in. smaller than nominal. Even though this difference was small, when multiplied by the number of specimens, the top specimen experienced an elevation reduction of 0.14 in. Although dimensional changes were less pronounced in S-1 through S-6, specimen elevations were adjusted based on pre-irradiation length measurements.

2. Thermal expansion.

   Thermal growth of the capsule wall and the graphite specimens also affected specimen position. Because the capsule and reactor are both made of similar material, their relative positions will not substantially change if they both experience the same reactor coolant temperature. However, the capsule wall temperature in the region of the core was an average of 102°C, while the reactor coolant was an average of 52°C. Thus, the core section of the capsule grew approximately 0.042 in., which placed the lower isolation weld plate 0.042 in. lower when the reactor was operating. The graphite specimens and holders, all of which sit on the lower isolation weld plate, experienced an average temperature of 611°C. As a result, the lower specimens experienced minimal thermal growth elevation change while the uppermost specimens had an upward thermal growth change of 0.20 in.

3. Shrinkage of specimens and specimen holders due to irradiation and load.

   All of the specimens and components in the AGC-2 test capsule experienced some degree of radiation-induced shrinkage. During the course of irradiation, neutron damage to the graphite specimens caused the specimens to shrink and move downward. In addition to irradiation effects, the compressed specimens in S-1 through S-6 and their supporting components were also subject to load-induced creep. Therefore, as the specimen elevation changed during the course of irradiation, there was a significant change in the specimen dose and, to a lesser extent, the specimen temperature.

The compressed specimen stacks had a graphite pushrod that applied a gas cylinder load. The top of the pushrod displacement was measured by a radiation-resistant linear variable differential transducer located 94 to 107 in. above the core mid-plane; its position was recorded throughout the test in the Nuclear Data Management and Analysis System. As seen in Figure 9, the response of the linear variable differential transducers and the specimen stack creep was nearly linear. Using this fact and the influences listed above, an average mid-cycle elevation for each specimen was calculated and reported for each reactor cycle. This average elevation was used to make accurate predictions of the specimen temperature and dose discussed below.

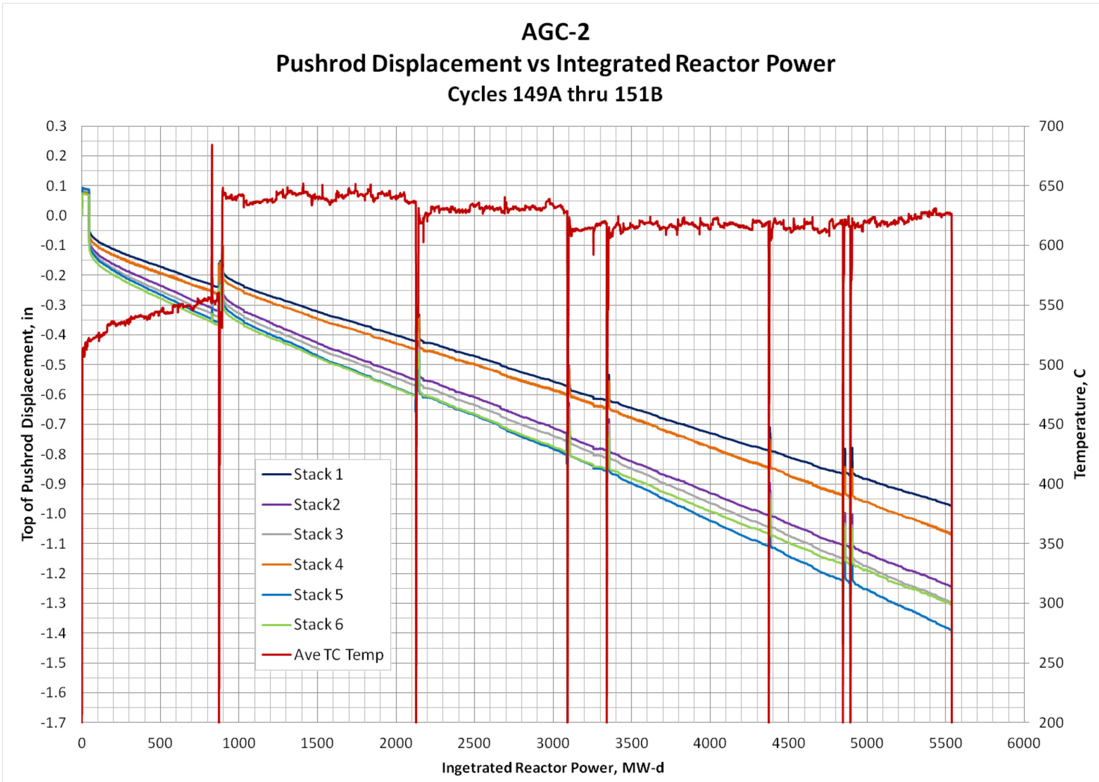

Figure 9. AGC-2 pushrod displacement.

A propagation of error analysis was performed to obtain an estimate of the uncertainty in the position values. This analysis took into consideration the uncertainties of all variables that make up the position calculation. The position is a function with the following variables:

$$Position = f(P, L_0, A, E, CTE, T, L_{End}) \tag{1}$$

where

P = applied load

L_0 = specimen pre-irradiated length

A = specimen cross-sectional area

E = specimen pre-irradiated Young's modulus

CTE = specimen pre-irradiated coefficient of thermal expansion

T = specimen temperature

L_{End} = specimen post-irradiated length.

The error in the position calculation of the specimens in the lower housing was not considered because they are not subjected to any load and, therefore, did not move as much as the specimens in the upper housing. The precision and accuracy of the dimensional (i.e., length and diameter), coefficient of thermal expansion, and Young's Modulus measurements were obtained from an inter-laboratory study between INL and Oak Ridge National Lab. Both the thermocouples' (manufactured by Idaho Laboratories

Corporation, ILC) and the load cells' (Honeywell Corp., Model 31/AL311CV) precision and accuracy were obtained from their respective manufacturer specifications.

Table 4 shows the precision and accuracy of each of the components that go into the position's overall uncertainty calculation. A root sum square of the individual elements was computed to provide a comprehensive uncertainty for the specimen position calculations. This gave a worst case uncertainty value for the position of a specimen within the experiment (the worst case being a specimen at the top of a compressed stack at the end of the experiment). This resulted in total uncertainty of ±4% of the position related to the reactor mid-plane.

Table 4. Precision and accuracy of position calculation variables and instrumentation.

	Precision (±%)	Accuracy (±%)
Pre-Irradiated Length	0.07	0.008
Post-Irradiated Length	0.07	0.008
Area	—	0.56
Thermal Growth	—	3.0
Young's Modulus	2.3	—
Temperature (ILC TCs)	—	1.0
Load Cell	0.3 [a]	0.05 [a]

a. Of full scale.

7. DOSE ANALYSIS

An as-run reactor physics analysis of the dose received by the AGC-2 capsule was performed in ECAR-2291 [13]. A Monte Carlo N-Particle (MCNP) transport code was used to model and calculate the as-run displacements per atom (dpa), the fast neutron flux (E > 0.1 MeV) and the heating rates (first cycle only) within the AGC-2 capsule. The heating rates were used to calculate the specimen stack temperatures (as discussed in Section 8). The dpa calculations were performed for each stack of specimens at 49 discrete elevations (in inches from reactor core mid-plane) throughout the experiment. The dpa tables reported in the ECAR are an accumulation of the dpa values through the end of each reactor cycle.

Using the accumulated dpa values from ECAR-2291 [13], dpa amounts were calculated for each individual cycle. This resulted in 35 data sets (i.e., seven stacks times five reactor cycles). A 6th order polynomial curve was applied through each of the 35 data sets. This provided a curve fit for each stack and every cycle. The total estimated accumulated dpa for a given specimen is then the sum of the evaluated dpa values for each cycle at the specimen's mid-cycle positions given in ECAR-2549 [12]. Figure A-1 in Appendix A shows a plot of the results of all curve fits by stack as a function of position in the capsule. Table 5 shows the resulting coefficients from the curve fitting described above. Figure 10 shows a diagram of how the specimen dpa was calculated from the MCNP run data.

Table 5. The dpa curve fit coefficients for each cycle and stack.

Cycle	Stack No.	a6	a5	a4	a3	a2	a1	a0
149A	1	7.2837E-10	1.2811E-08	-5.2488E-07	-7.4389E-06	-1.0393E-03	-1.0566E-03	8.0576E-01
149A	2	6.9695E-10	1.0113E-08	-4.6034E-07	-5.6438E-06	-1.0296E-03	-1.1854E-03	7.7612E-01
149A	3	4.5906E-10	1.1801E-08	-2.2051E-07	-6.8585E-06	-9.7610E-04	-7.9748E-04	6.9296E-01
149A	4	4.8008E-10	9.7006E-09	-2.2962E-07	-5.1520E-06	-9.0851E-04	-1.0133E-03	6.4224E-01
149A	5	4.6682E-10	8.5818E-09	-2.2769E-07	-4.2802E-06	-9.8218E-04	-1.2638E-03	6.9572E-01
149A	6	6.2628E-10	1.1245E-08	-4.0055E-07	-6.0865E-06	-1.0402E-03	-1.2967E-03	7.7712E-01

Table 5. (continued).

Cycle	Stack No.	a6	a5	a4	a3	a2	a1	a0
149A	7	5.5614E-10	8.1201E-09	-3.1877E-07	-3.8087E-06	-1.0084E-03	-1.4563E-03	7.3351E-01
149B	1	1.3551E-09	1.5014E-08	-1.0338E-06	-8.5283E-06	-1.4196E-03	-1.7074E-03	1.1509E+00
149B	2	7.5796E-10	1.3628E-08	-4.2456E-07	-7.3019E-06	-1.5298E-03	-1.8316E-03	1.1138E+00
149B	3	7.3973E-10	1.3389E-08	-3.7667E-07	-6.9812E-06	-1.3848E-03	-1.6202E-03	9.9177E-01
149B	4	7.7042E-10	1.1088E-08	-3.9734E-07	-5.8395E-06	-1.2812E-03	-1.4394E-03	9.1605E-01
149B	5	7.7425E-10	1.2700E-08	-3.9695E-07	-7.2789E-06	-1.3892E-03	-1.3214E-03	9.9207E-01
149B	6	1.0615E-09	1.4868E-08	-7.2593E-07	-8.2242E-06	-1.4393E-03	-1.6101E-03	1.1043E+00
149B	7	7.0035E-10	1.4527E-08	-3.6619E-07	-8.2046E-06	-1.4577E-03	-1.3803E-03	1.0492E+00
150B	1	1.0146E-09	1.2741E-08	-9.2105E-07	-7.3689E-06	-1.0140E-03	-1.2763E-03	8.9768E-01
150B	2	9.9886E-10	1.2354E-08	-8.3522E-07	-6.9698E-06	-1.0117E-03	-1.2707E-03	8.6237E-01
150B	3	7.2928E-10	9.5350E-09	-5.3704E-07	-5.2863E-06	-9.7297E-04	-1.1664E-03	7.6927E-01
150B	4	6.0749E-10	1.0705E-08	-4.3067E-07	-5.9250E-06	-9.2283E-04	-1.0011E-03	7.1241E-01
150B	5	8.8570E-10	1.0368E-08	-6.8492E-07	-5.7426E-06	-9.4176E-04	-1.2013E-03	7.6944E-01
150B	6	8.9888E-10	1.0963E-08	-7.2304E-07	-5.8688E-06	-1.0460E-03	-1.4960E-03	8.6382E-01
150B	7	8.5398E-10	9.8911E-09	-6.5854E-07	-5.4793E-06	-1.0072E-03	-1.2881E-03	8.1618E-01
151A	1	1.0448E-09	1.3578E-08	-8.1914E-07	-7.7176E-06	-1.1337E-03	-1.3092E-03	9.3234E-01
151A	2	1.1293E-09	1.4996E-08	-9.2033E-07	-8.3851E-06	-1.2047E-03	-1.4243E-03	1.0070E+00
151A	3	1.1472E-09	1.5817E-08	-1.0241E-06	-9.0650E-06	-1.2976E-03	-1.5990E-03	1.1228E+00
151A	4	1.2799E-09	1.8983E-08	-1.2260E-06	-1.1775E-05	-1.2723E-03	-1.2029E-03	1.1645E+00
151A	5	1.3416E-09	1.7793E-08	-1.2329E-06	-1.0893E-05	-1.2407E-03	-1.2413E-03	1.1204E+00
151A	6	1.0422E-09	1.2318E-08	-8.6321E-07	-6.5223E-06	-1.2058E-03	-1.6834E-03	1.0044E+00
151A	7	1.1045E-09	1.6001E-08	-9.6247E-07	-9.0137E-06	-1.2390E-03	-1.5121E-03	1.0619E+00
151B	1	7.7567E-10	1.3200E-08	-5.3316E-07	-7.5967E-06	-1.0956E-03	-1.0754E-03	8.4439E-01
151B	2	1.0998E-09	1.0352E-08	-8.1264E-07	-5.1945E-06	-1.1243E-03	-1.6888E-03	9.0640E-01
151B	3	1.2964E-09	1.2936E-08	-1.0725E-06	-7.3239E-06	-1.1592E-03	-1.5090E-03	1.0038E+00
151B	4	1.2852E-09	9.2715E-09	-1.1748E-06	-5.1742E-06	-1.1506E-03	-1.8932E-03	1.0457E+00
151B	5	9.9049E-10	1.3004E-08	-8.5178E-07	-7.4535E-06	-1.2167E-03	-1.5341E-03	1.0189E+00
151B	6	9.9035E-10	1.4245E-08	-7.7834E-07	-7.8859E-06	-1.1184E-03	-1.3018E-03	9.1206E-01
151B	7	5.7700E-10	9.3612E-09	-4.4200E-07	-4.0913E-06	-1.2384E-03	-2.0826E-03	9.6035E-01

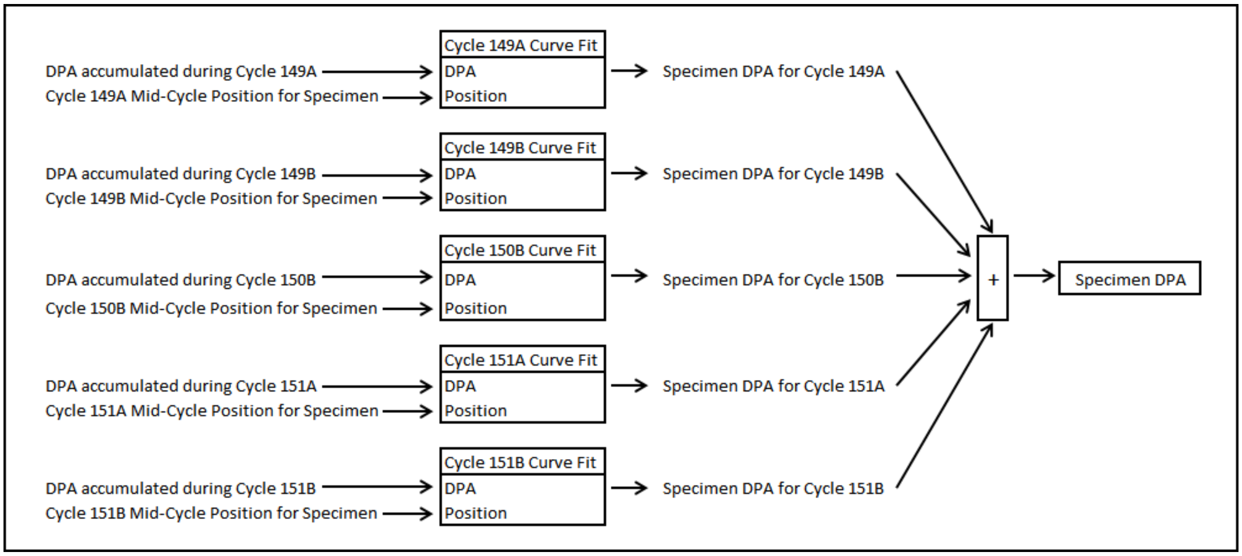

Figure 10. Specimen dpa calculation diagram.

7.1 Uncertainty in Displacements per Atom Calculations

Uncertainties exist at every step of the calculation and measurement process used in determining the dpa in the AGC experiment. Some uncertainties contribute very little to output uncertainties (e.g., experiment geometry dimensions), while others have large impacts (e.g., power measurement). The uncertainty of the determined fast fluence within the graphite samples was dominated by model uncertainty. The data assimilation process, where experimental flux wire results were combined with the results of the high fidelity simulations, relied heavily on the model results because only two data points were determined experimentally, whereas the model provided 100s of data points. The sources and determined values of uncertainties for the determined AGC dpa are described in the following subsections.

7.2 Flux Wire Spectral Measurements (AGC-2) Uncertainties

The radiation counting process contributed little uncertainty to the total dpa calculations; however, long decay times between irradiation and measurement made it difficult to collect all relevant data. The uncertainties in the ^{54}Mn and ^{94}Nb measurements were 3% in every case. Only one of the two ^{46}Sc measurements detected ^{46}Sc and the ^{46}Sc measurement had an uncertainty of 8%. No data were obtained for ^{93m}Nb or ^{59}Fe. Detection of ^{93m}Nb requires measuring a low-energy x-ray. To do so, the wire must be dissolved and deposited on a very thin film prior to counting, but this dissolution was not performed for AGC-2. ^{59}Fe data appear to have been lost since about 17 half-lives elapsed between the end of irradiation on May 5, 2012, and the measurements that were performed in June and July 2014.

7.3 Spectral Adjustment Uncertainties

A series of corrections were applied to the measured activation product inventories in the SigPhi calculator to obtain saturated $\sigma\varphi$ values [14]. Gamma self-absorption reduced the measured activity by about 1% for both wires and neutron burnup varied from 3 to 8% depending on position. In addition to the corrections determined by the SigPhi calculator and ancillary codes in the STAYSL Pacific Northwest National Laboratory (PNNL) suite, we applied one additional correction to account for shielding from the vanadium capsule (i.e., the AGC-2 flux wires were not removed from this capsule prior to counting because they were at PNNL for AGC-1) [14]. Using the estimated average thickness of the capsule that was based on its size and mass (0.01 in.) and mass attenuation coefficients for vanadium at the appropriate incident gamma energy, this is also an approximate 1% effect.

The computed $\sigma\varphi$ values were provided to STAYSL PNNL, along with a height-averaged MCNP spectrum, and the cross-section data distributed with the code. Because overall uncertainty in the MCNP value was not known, we used the values in Table 6, based on past precedent alone [15]. The resulting fast fluences were plotted versus height in Figure 11.

Table 6. MCNP uncertainties input to STAYSL PNNL.

Energy (MeV)		Uncertainty
Lower	Upper	—
—	9.9e-11	90%
9.9e-11	1.0e-3	30%
1.0e-3	1.0e-2	20%
1.0e-2	1.5	15%
1.5	20.1	15%

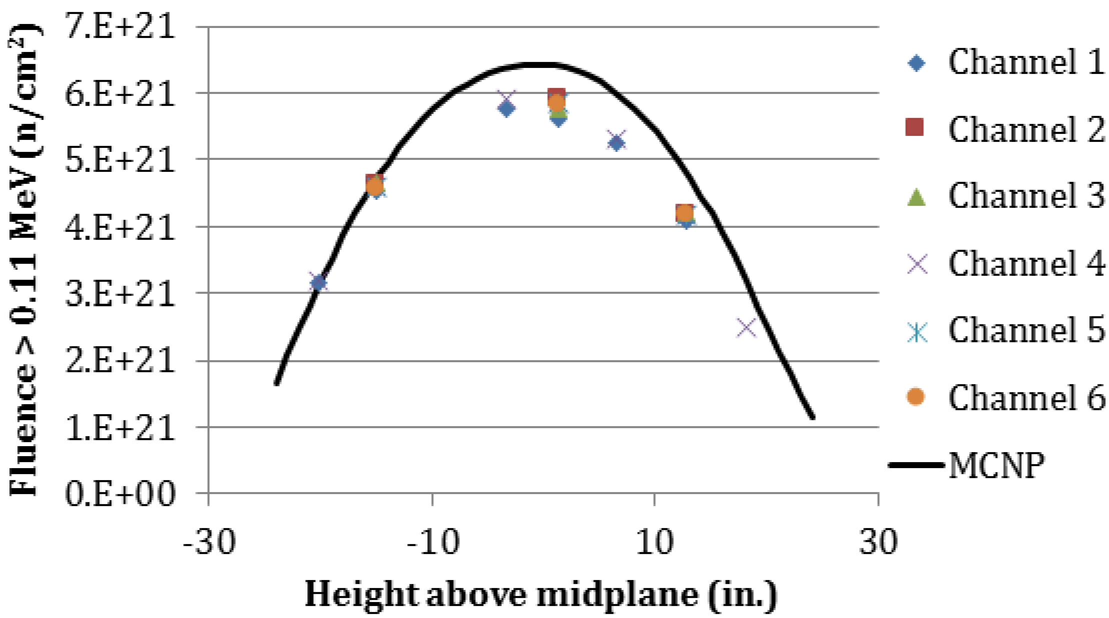

Figure 11. Fast fluence versus position as determined from AGC-2 flux wire analysis and comparison with pre-test MCNP predictions [12].

7.4 Monte Carlo N Particle/ORIGEN Model Uncertainties

The uncertainty of the determined fast fluence within the graphite samples was dominated by model uncertainty. The MCNP input consisted of a very large number of parameters that included the reactor geometry, material loadings, and operational data such as power, control drum, and neck shim positions. These parameters contained approximations or measurement uncertainties such that the relevant outputs were uncertain. Furthermore, the actual calculation process was Monte Carlo based, which added another source of uncertainty. Table 7 lists relevant model inputs with their estimated impact on final results. The relevant output for these studies will be the energy-dependent axial flux in each of the graphite samples within the AGC experiment.

Model uncertainty arises from model approximations and measurement uncertainties. Specifically, model approximations can lead to biases in the neutron flux (energy and space dependent). For example, modeling the fuel assemblies as homogenized regions could increase resonance capture rates, reducing the thermal flux (i.e., increasing the fast flux), which leads to the experiment interacting with the wrong energy dependence in the flux. Furthermore, as-run power measurements are used to normalize lobe powers. These lobe powers determine the normalization factors for the flux within the AGC experiment and are inputs for fuel burnup calculations. The normalization factors contribute directly to result uncertainties and the fuel burnup calculations can indirectly affect results.

Table 7. Model uncertainties sources.

Model Input	Notional Impact on Results	Notes
Explicit modeling of fuel geometry	Low	Local flux possibly not captured by homogenization
Estimated source used instead of eigenvalue flux	Low	Increased uncertainty introduced through burnup
Control element positions near the experiment	Medium	Large changes in flux possible
Material temperatures	Low	Doppler broadening in cross sections
Fuel loading	Medium	Fresh fuel and fission product buildup
Tally normalization factors (Q-value)	Low	Total energy from fission difficult to know exactly
Random number seed	Medium	Single Monte Carlo calculations tend to underpredict result uncertainties
Nuclear data	Low	Physical neutron interaction data contain uncertainties
As-run power measurements	Medium	Difficult to measure lobe powers; detectors have inherent uncertainty
Key:		
Low: 0 to 5%	Medium: 5 to 10%	High: 10+%

7.5 Future Work

While uncertainties for both the flux wire measurements and cross sections are readily available, it is more difficult to estimate it for the MCNP input spectrum. This includes not only statistical uncertainty inherent in the Monte Carlo calculation, but any other error resulting from simplifications in geometry. Therefore, the total MCNP uncertainty is difficult to quantify; our present conservative estimate is that it is large relative to the other sources of error and, therefore, contributes disproportionately to the overall error in the radiation damage estimate. For this reason, it is of interest to assess the MCNP uncertainty in a more rigorous and quantitative way.

Currently, no uncertainties are tracked or calculated. It is not possible to track uncertainty through the calculations given the current computer programs, without drastic modifications to the codes. It is possible to calculate the effects of model inputs on model outputs, but this is not currently performed because of limited resources and lack of proper methodology. Though uncertainties in results are not calculated, it is known that uncertainties exist and must be estimated. To accomplish this, an estimated factor that is based loosely on expert opinion is used. A future objective is to quantify this uncertainty based on actual input uncertainty.

8. THERMAL ANALYSIS

A finite element, steady-state heat transfer analysis of the AGC-2 test train was performed using ABAQUS software. This analysis, documented in ECAR-2322 [16], calculated an elevational temperature for each specimen stack at a minimum of three selected times in each reactor cycle. These calculation points were derived from reactor power data, helium-argon gas gap flows through the specimen stacks, as-run heating rates, and as-run graphite dose (i.e., dpa) values. Only a summary of how the average specimen temperature was calculated is contained here. ECAR-2322 describes the model in greater detail; therefore, the reader who requires a technical and complete understanding of the specimen temperature determination should refer to the ECAR.

Figure 12 shows the measured thermocouple temperatures over the course of the experiment. Analyses were conducted on correlations between thermocouple temperatures and differences between thermocouple temperatures to look for trends and step changes that might indicate thermocouple degradation or drift. Correlation analysis was used to identify instances when thermocouples form short circuits (referred to as virtual junctions), which result in thermocouples reporting temperatures from some location in the capsule other than the location where they are intended to read. No evidence was found for virtual junctions. Control charts for differences between thermocouples were used to identify instances when one thermocouple changes its behavior relative to the other thermocouples. No instances were found where a thermocouple significantly and uniformly changed behavior relative to the other thermocouples [17].

Because of the fact that no thermocouple drift was identified, the parameters of the thermal model were adjusted to minimize the difference between the measured thermocouple values and calculated temperatures. After the final adjustments to the model were made, temperatures were calculated at 57 distinct elevations for Stacks 1 through 6 and 170 elevations for Stack 7 on 3 or 4 selected days in every cycle. Figure 13 shows the results of the calculated temperatures from the model versus the thermocouple measurements for TC-01 for all of the reactor cycles.

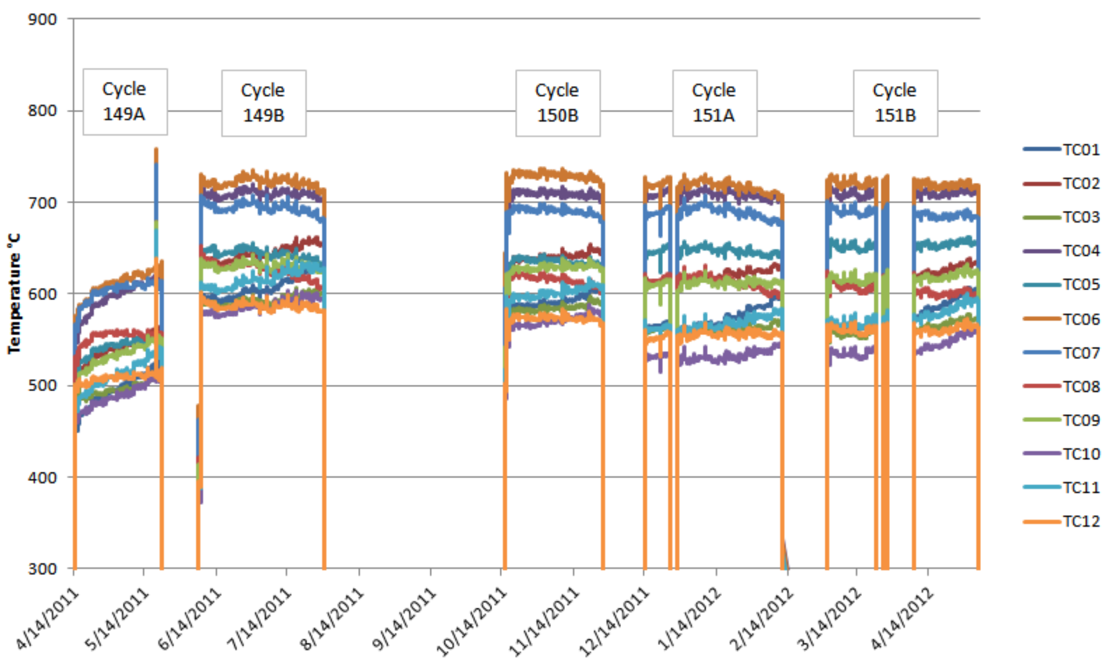

Figure 12. Time history of thermocouple data during the AGC-2 capsule.

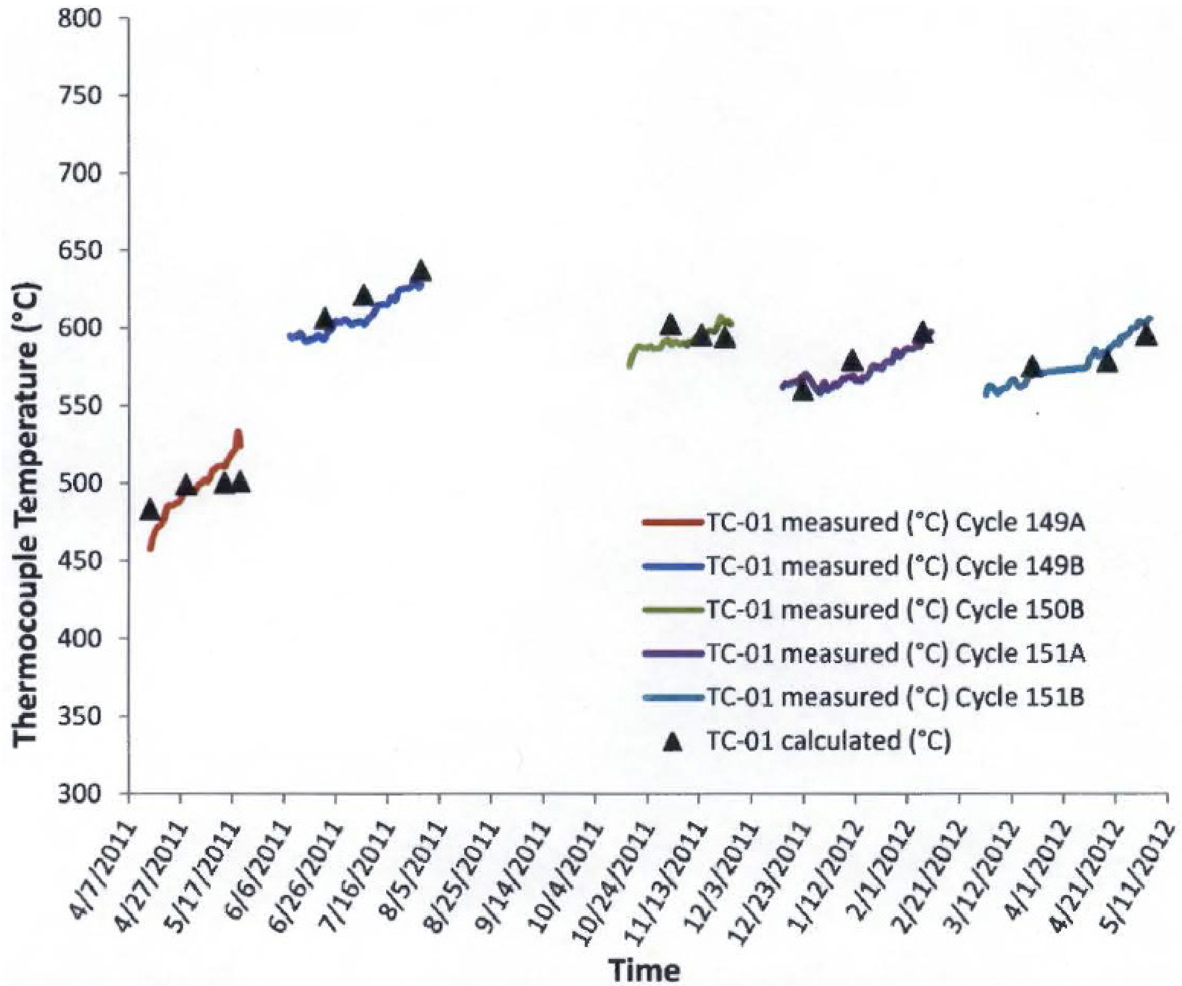

Figure 13. Measured and calculated temperature of TC-01 during all irradiation cycles.

Using the calculated output temperatures of the thermal model, average temperature curves for every specimen stack were computed for each of the reactor cycles. Curve fits were then applied to each of the stack's cycle averages (Figure 14). This resulted in 35 sets of curve fit coefficients (seven stacks times five reactor cycles). Ninth order polynomials were used for each of the stacks:

$$T = a_9x^9 + a_8x^8 + a_7x^7 + a_6x^6 + a_5x^5 + a_4x^4 + a_3x^3 + a_2x^2 + a_1x + a_0, \quad (2)$$

where

T = temperature (°C)

x = elevation (inches)

$a_9 - a_0$ = curve fit coefficients (shown in Table 8).

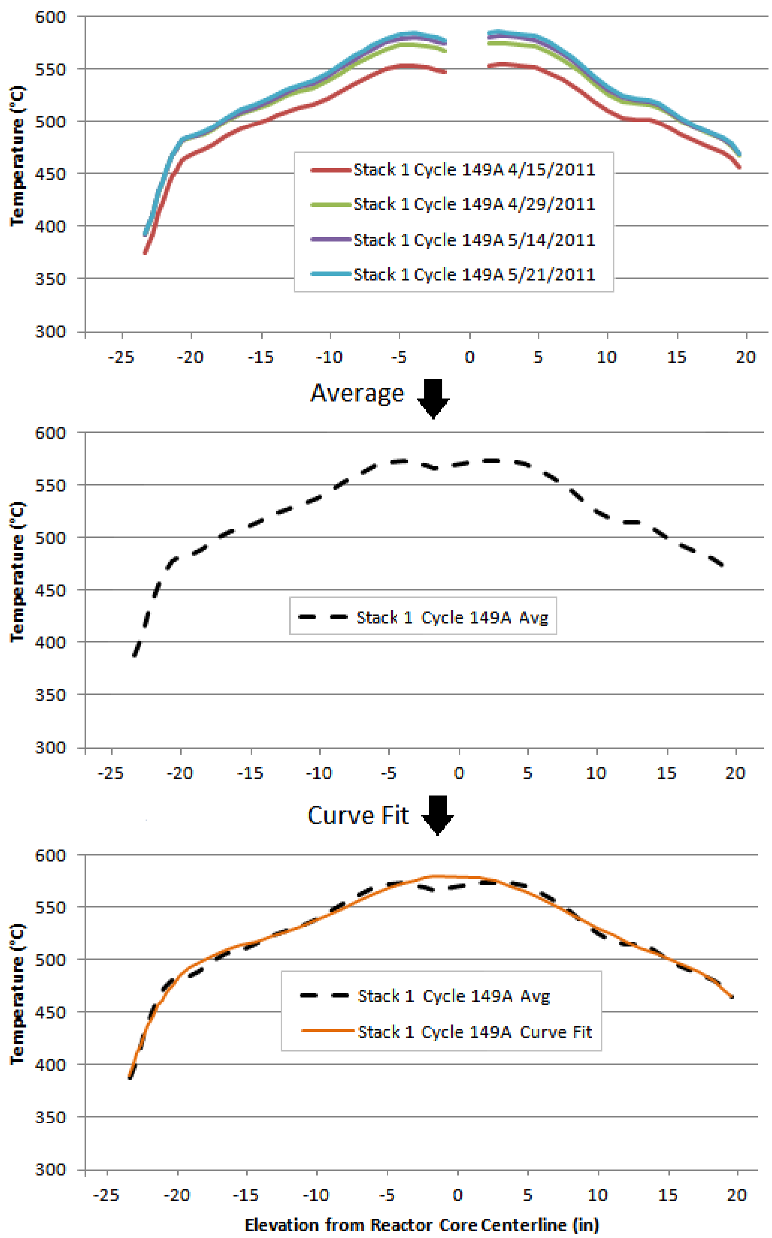

Figure 14. Stack 1, Cycle 149A temperature averaging and curve fit.

Higher order curve fit polynomials were needed in particular for Stack 7, where there is a dramatic temperature increase in the upper elevations (i.e., greater than 17 inches) of the stack. This increase was due to a tungsten heat generation cap incorporated into the design. Table 8 shows the curve fit coefficients for each cycle and each stack.

The 35 curve fits were used to evaluate temperature for every specimen's mid-cycle positions that were given in ECAR-2549 [12]. Thus, for every specimen, a temperature value was calculated for each of the cycles. To obtain an estimation of a specimen's temperature over the entire duration of the experiment, the cycle temperatures were weighted by the number of MW-days and averaged. The complete averaging scheme is summarized in Figure 15.

Table 8. Temperature curve fit coefficients for each cycle and stack.

Cycle	Stack No.	a9	a8	a7	a6	a5	a4	a3	a2	a1	a0
149A	1	1.3146E-10	-8.3862E-09	-2.1831E-07	4.8767E-06	9.7711E-05	-2.7462E-04	-1.4573E-02	-4.0454E-01	9.5588E-02	5.7592E+02
149A	2	8.4941E-11	-9.5547E-09	-1.7345E-07	5.8863E-06	8.2300E-05	-5.5053E-04	-1.2691E-02	-3.7893E-01	1.0567E-01	5.7447E+02
149A	3	1.6859E-11	-1.0754E-08	-1.0451E-07	6.9909E-06	5.9688E-05	-8.7308E-04	-1.0534E-02	-3.4968E-01	1.8837E-01	5.7437E+02
149A	4	1.3957E-11	-1.0091E-08	-9.3336E-08	6.4022E-06	5.4361E-05	-6.8893E-04	-1.0150E-02	-3.7321E-01	2.6518E-01	5.7554E+02
149A	5	5.4585E-11	-9.1003E-09	-1.3064E-07	5.4458E-06	6.4875E-05	-3.6285E-04	-1.0631E-02	-4.2151E-01	1.3126E-01	5.7875E+02
149A	6	9.3398E-11	-8.8380E-09	-1.7707E-07	5.2633E-06	8.2844E-05	-3.5106E-04	-1.2659E-02	-4.1520E-01	4.4961E-02	5.7941E+02
149A	7	2.3061E-10	-1.1160E-09	-5.0643E-08	3.4387E-06	4.0181E-06	-6.8585E-04	-2.3502E-03	-3.6765E-01	-1.3264E-01	6.0362E+02
149B	1	5.6549E-10	8.4266E-09	-6.4638E-07	-1.2118E-05	2.6964E-04	5.2340E-03	-4.9410E-02	-9.8682E-01	3.4204E+00	6.8894E+02
149B	2	5.1215E-10	7.0708E-09	-5.9506E-07	-1.0946E-05	2.5198E-04	4.9135E-03	-4.7213E-02	-9.5721E-01	3.4214E+00	6.8732E+02
149B	3	4.3986E-10	5.8029E-09	-5.2108E-07	-9.7673E-06	2.2740E-04	4.5664E-03	-4.4820E-02	-9.2569E-01	3.5101E+00	6.8726E+02
149B	4	4.3641E-10	6.5322E-09	-5.0849E-07	-1.0412E-05	2.2148E-04	4.7667E-03	-4.4414E-02	-9.5111E-01	3.5989E+00	6.8856E+02
149B	5	4.8269E-10	7.6862E-09	-5.5062E-07	-1.1517E-05	2.3331E-04	5.1397E-03	-4.4973E-02	-1.0057E+00	3.4529E+00	6.9216E+02
149B	6	5.2684E-10	8.0568E-09	-6.0268E-07	-1.1793E-05	2.5333E-04	5.1754E-03	-4.7239E-02	-1.0011E+00	3.3598E+00	6.9296E+02
149B	7	1.0790E-09	2.9046E-08	-6.3174E-07	-2.1043E-05	1.7428E-04	6.0722E-03	-3.2962E-02	-1.0144E+00	2.9507E+00	7.2054E+02
150B	1	1.4590E-09	3.4221E-08	-1.3346E-06	-3.4330E-05	4.2715E-04	1.1554E-02	-5.7273E-02	-1.6759E+00	2.2452E+00	7.0642E+02
150B	2	1.4046E-09	3.2825E-08	-1.2825E-06	-3.3126E-05	4.0929E-04	1.1225E-02	-5.5052E-02	-1.6453E+00	2.2459E+00	7.0476E+02
150B	3	1.3329E-09	3.1587E-08	-1.2086E-06	-3.1965E-05	3.8464E-04	1.0881E-02	-5.2651E-02	-1.6139E+00	2.3359E+00	7.0470E+02
150B	4	1.3292E-09	3.2304E-08	-1.1960E-06	-3.2605E-05	3.7878E-04	1.1082E-02	-5.2241E-02	-1.6395E+00	2.4231E+00	7.0603E+02
150B	5	1.3752E-09	3.3441E-08	-1.2384E-06	-3.3705E-05	3.9086E-04	1.1457E-02	-5.2855E-02	-1.6949E+00	2.2800E+00	7.0967E+02
150B	6	1.4208E-09	3.3831E-08	-1.2919E-06	-3.3993E-05	4.1139E-04	1.1494E-02	-5.5196E-02	-1.6902E+00	2.1892E+00	7.1046E+02
150B	7	2.1761E-09	6.2132E-08	-1.4014E-06	-4.7707E-05	3.3334E-04	1.3217E-02	-3.9295E-02	-1.7503E+00	1.7175E+00	7.3869E+02
151A	1	7.3657E-10	1.2433E-08	-8.0189E-07	-1.5362E-05	3.2339E-04	6.3659E-03	-5.6999E-02	-1.2615E+00	3.3325E+00	6.8639E+02
151A	2	6.8483E-10	1.1140E-08	-7.5194E-07	-1.4247E-05	3.0615E-04	6.0614E-03	-5.4857E-02	-1.2334E+00	3.3326E+00	6.8485E+02
151A	3	6.1225E-10	9.8486E-09	-6.7851E-07	-1.3055E-05	2.8203E-04	5.7118E-03	-5.2523E-02	-1.2014E+00	3.4173E+00	6.8477E+02
151A	4	6.0928E-10	1.0552E-08	-6.6684E-07	-1.3677E-05	2.7653E-04	5.9058E-03	-5.2165E-02	-1.2261E+00	3.5045E+00	6.8603E+02
151A	5	6.5682E-10	1.1714E-08	-7.1036E-07	-1.4789E-05	2.8888E-04	6.2792E-03	-5.2819E-02	-1.2800E+00	3.3683E+00	6.8949E+02
151A	6	6.9784E-10	1.2027E-08	-7.5905E-07	-1.5013E-05	3.0769E-04	6.3009E-03	-5.4950E-02	-1.2744E+00	3.2791E+00	6.9025E+02
151A	7	1.3542E-09	3.6983E-08	-8.4615E-07	-2.7143E-05	2.3601E-04	7.8434E-03	-4.0726E-02	-1.3332E+00	2.9024E+00	7.1732E+02
151B	1	7.5186E-10	1.4289E-08	-8.4959E-07	-1.7260E-05	3.7000E-04	6.9942E-03	-7.3478E-02	-1.3430E+00	5.1506E+00	6.9588E+02
151B	2	6.9824E-10	1.2979E-08	-7.9750E-07	-1.6127E-05	3.5197E-04	6.6843E-03	-7.1223E-02	-1.3144E+00	5.1453E+00	6.9433E+02
151B	3	6.2742E-10	1.1705E-08	-7.2583E-07	-1.4950E-05	3.2844E-04	6.3395E-03	-6.8963E-02	-1.2831E+00	5.2316E+00	6.9427E+02

Table 8. (continued).

Cycle	Stack No.	a9	a8	a7	a6	a5	a4	a3	a2	a1	a0
151B	4	6.2268E-10	1.2356E-08	-7.1308E-07	-1.5534E-05	3.2273E-04	6.5240E-03	-6.8579E-02	-1.3068E+00	5.3169E+00	6.9551E+02
151B	5	6.6862E-10	1.3502E-08	-7.5476E-07	-1.6630E-05	3.3439E-04	6.8923E-03	-6.9145E-02	-1.3602E+00	5.1791E+00	6.9895E+02
151B	6	7.1447E-10	1.3933E-08	-8.0758E-07	-1.6949E-05	3.5445E-04	6.9393E-03	-7.1436E-02	-1.3567E+00	5.0972E+00	6.9973E+02
151B	7	1.4594E-09	4.1690E-08	-9.3856E-07	-3.0912E-05	2.8667E-04	8.8577E-03	-5.6757E-02	-1.4415E+00	4.6911E+00	7.2703E+02

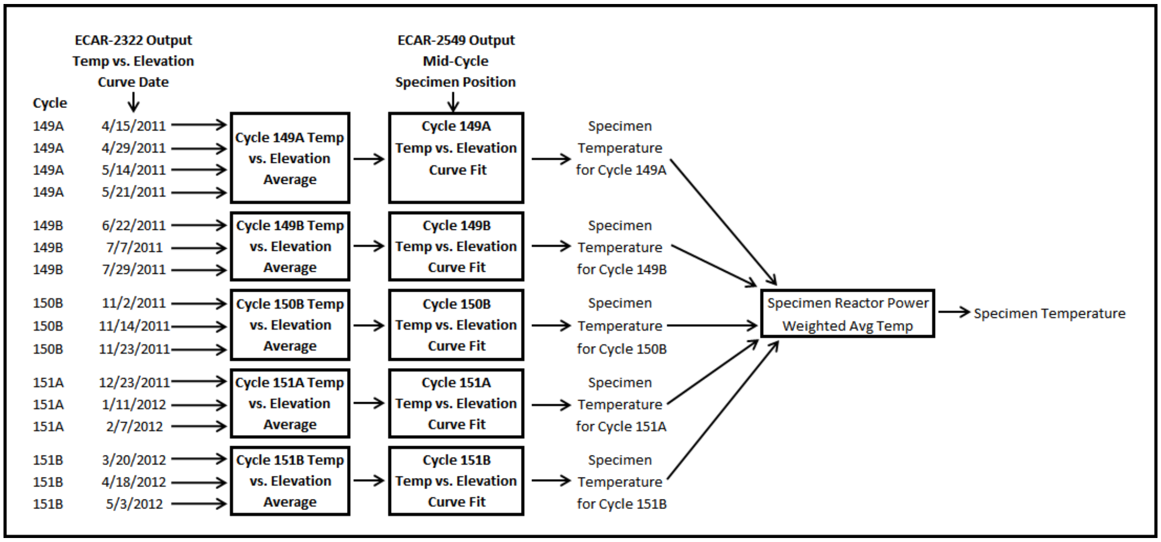

Figure 15. Specimen stack temperature averaging.

The accuracy of the temperature model developed by the ABAQUS software was validated by comparing the calculated temperatures to the thermocouple values measured and recorded in the Nuclear Data Management and Analysis System. In particular, the mean of the temperature difference indicated the bias in the temperature calculation, and the standard deviation of the temperature difference indicated the variability in the temperature calculation. The uncertainty in the calculation was estimated to be equal to:

$$\mu \pm 2 \times \sigma, \tag{3}$$

where

μ = the mean of the temperature difference

σ = the standard deviation of the temperature difference.

Therefore, the maximum uncertainty of the temperature model is ±40°C. ECAR-3017 provides a complete explanation of the uncertainty calculations of the temperature model [18].

In addition to the uncertainty in the temperature model, the individual specimen temperatures also have error associated with the curve fitting. The curve fitting error was quantified by computing the cumulative deviation of the temperature data from the curve fit line. It is reported here as a percentage with respect to the stack average (across all specimen positions). Overall, these errors were much less than the errors associated with the temperature model (i.e., less than 2%). The largest of the curve fitting errors occurred during reactor Cycle 149A and are shown in Table 9.

Table 9. Curve fitting standard deviations for reactor Cycle 149A.

	Stack Average (°C)	**Standard Deviation about the Regression (°C)**	**Regression Coefficient of Variance (%)**
Stack 1	510	3.55	0.70
Stack 2	510	3.51	0.69
Stack 3	510	3.42	0.67
Stack 4	510	3.39	0.67
Stack 5	511	3.41	0.67
Stack 6	512	3.48	0.68
Stack 7	549	8.40	1.53

9. LOAD ANALYSIS

All specimens in the upper portions of Stacks 1 through 6 were loaded using pneumatic load cylinders. The nominal loads used for each stack were 400 lbf for Stacks 1 and 4, 500 lbf for Stacks 2 and 5, and 600 lbf for Stacks 3 and 6. These nominal loads equated to stresses of approximately 2,000 psi, 2,500 psi, and 3,000 psi on the 0.5-in. diameter specimens. Radial irradiation dimensional change was considered to be very small; therefore, any lateral shrinkage or expansion during irradiation was ignored. The matching loads were arranged diametrically opposite in the capsule to minimize eccentric loading on the specimen holders. Load analysis for the AGC-2 capsule was documented in ECAR-2925 [19] and the results are shown in Table 10. Figure 16 shows that the loads were applied relatively constant during the course of irradiation.

Table 10. Load values after application of threshold for each stack.

	Stack 1	Stack 2	Stack 3	Stack 4	Stack 5	Stack 6
Average (lbf)	406	508	606	395	503	604
Two times standard deviation (lbf)	11	13	12	9	7	10
Coefficient of variance (%)	1.3	1.3	1.0	1.1	0.7	0.8

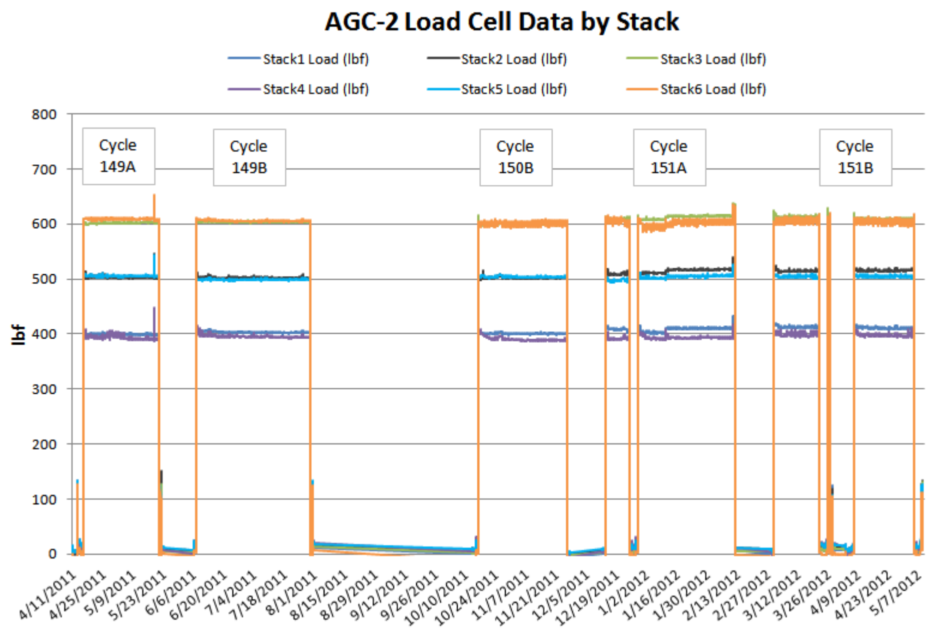

Figure 16. Compressive loads for each specimen stack over the duration of the AGC-2 capsule.

After analyzing the power and load history data, it was determined that there were periods of time (at the start of cycles) where there was reactor power but no load being applied to the stacks. The load averaging (in ECAR-2925 [19]) took this into account by only averaging load data during periods of time when the reactor was outputting power. The logic used for the load calculations was as follows: if the load was greater than 90% of the nominal load and the reactor power was greater than 2 MW, then that data point was included in the average load calculation for the stack.

The precision of the load data was measured by calculating the standard deviation. To compare precision among the stacks with different nominal loads, the coefficient of variation was calculated. The range of these coefficients of variation was between 0.7% (Stack 5) and 1.3% (Stacks 1 and 2). The magnitudes of the coefficients of variation were all on the same order, indicating the consistency between stack loads and good repeatability with each stack. The accuracy of the data was quantified from the specifications of the load cells used in the experiment. The load cells used have an accuracy of ±0.3% of full-scale reading. Full scale of the load cells is 1,000 lbf; therefore, the accuracy is ±3 lbf.

10. TABLE OF ADJUSTED DOSE, TEMPERATURE, AND LOAD

The position of the individual specimens in the reactor changed due to irradiation damage, stress-induced creep, and thermal expansion. Table B-1 through Table B-18, in Appendix B, show the results of the temperature, dose, and load calculations as they correlate to each specimen and its adjusted position in the AGC-2 capsule. These data reflect the average change in elevation the specimens experienced over the duration of the experiment and will be used in future analysis of AGC-2 creep and property data.

11. REFERENCES

[1] ORNL, 2013, *AGC-1 Specimen Post Irradiation Data Report*, ORNL/TM-2013/242, Oak Ridge National Laboratory, September 2013.

[2] Burchell, T., R. Bratton, and W. Windes, 2007, *NGNP Graphite Selection and Acquisition Strategy*, ORNL/TM-2007/153, Oak Ridge National Laboratory, September 2007.

[3] Bratton, R. L. and T. D. Burchell, 2005, *NGNP Graphite Testing and Qualification Specimen Selection Strategy*, INL/EXT-05-00269, Idaho National Laboratory, May 2005.

[4] INL, *Graphite Technology Development Plan*, INL/EXT-07-13165, Revision 0, Idaho National Laboratory, September 2007.

[5] PLN-2497, 2010, “Graphite Technology Development Plan,” Revision 1, Idaho National Laboratory, October 2010.

[6] TFR-645, 2010, “Advanced Graphite Capsule AGC-2 Experiment Test Train,” Revision 0, July 2010.

[7] DWG 600786, “ATR Advanced Graphite Capsule (AGC-2) Graphite Specimen Machining Details,” Revision 2, Idaho National Laboratory, July 9, 2012.

[8] DWG 601256, “Advanced Graphite Capsule 2 (AGC-2) Specimen Stack-Up Arrangements,” Revision 1, Idaho National Laboratory, July 2012.

[9] DWG 601266, “ATR Advanced Graphite Capsule Number 2 (AGC-2) Capsule Facility Assemblies,” Revision 2, Idaho National Laboratory, July 2012.

[10] INL, *Engineering Work Instructions for Assembling the AGC-2 Experiment*, WO 137268-01.

[11] Windes, W. E., P. L. Winston, and W.D. Swank, 2014, *AGC-2 Disassembly Report*, INL/EXT-14-32060, May 2014.

[12] Reed, Ted, “AGC-2 Individual Specimen Position Adjustment,” ECAR-2549, Idaho National Laboratory, June 2016.

[13] Parry, J. R., 2014, “As-Run Physics Analysis for the AGC-2 Experiment Irradiated in the ATR,” ECAR-2291, Idaho National Laboratory, March 6, 2014.

[14] L. R. Greenwood and C. D. Johnson, “User Guide for the STAYSL PNNL Suite of Software Tools,” PNNL-22253, February 2013.

[15] Greenwood, L. R., 2012, “Analysis of AGC-1 Neutron Fluence Monitors,” PNNL Project 23747, August 2012.

[16] Murray, Paul, “As-Run Thermal Analysis Of The AGC-2 Experiment,” ECAR-2322, Idaho National Laboratory, April 2014.

[17] INL, *AGC-2 Irradiation Data Qualification Final Report*, INL/EXT-12-26248, Idaho National Laboratory, July 2012.

[18] Murray, Paul, “Uncertainty Analysis Of Temperature In The AGC-1 And AGC-2 Experiments,” ECAR-3017, Idaho National Laboratory, April 2016.

[19] Rohrbaugh, David, “AGC-2 Specimen Load Calculations by Stack”, ECAR-2925, Idaho National Laboratory, February 2016.

Appendix A
Three-Dimensional Dose Plot

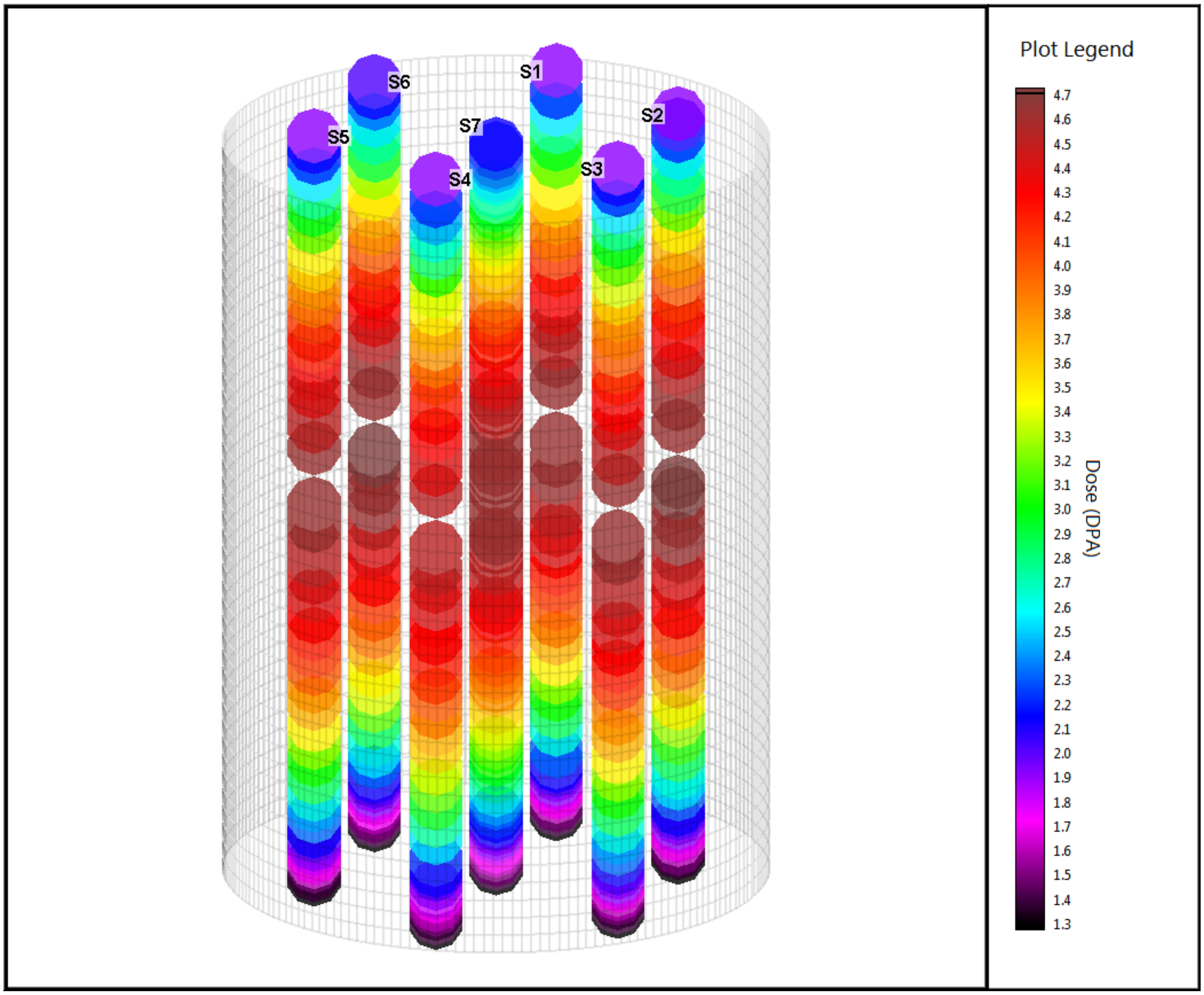

Figure A-1. Three-dimensional plot of the specimen dose as a function of position in the AGC capsule.

Appendix B
Tabulation of Specimen Position, Load, Dose, and Temperature

Table B-1. Stack 1 compressed.

Loading Order	Specimen ID	Graphite Grade	Nominal Specimen Elevation (in)	End of Test Specimen Elevation (in)	Specimen Temperature (°C)	Specimen Dose (DPA)	Stack Load (lbf)
23	CW1 01	H-451	19.500	18.873	541	2.0	406
22	1A	Flux Monitor	18.875	18.259	549	2.2	406
21	DW1 01	PCEA	18.250	17.645	556	2.3	406
20	BW1 01	NBG-18	17.250	16.662	566	2.6	406
19	EW01 02	IG-110	16.250	15.681	573	2.8	406
18	FW01 01	IG-430	15.250	14.701	579	3.0	406
17	DW1 02	PCEA	14.250	13.723	583	3.2	406
16	AY	Flux Monitor	13.625	13.111	586	3.3	406
15	BW1 02	NBG-18	13.000	12.497	589	3.5	406
14	FW01 02	IG-430	12.000	11.518	594	3.6	406
13	EW01 04	IG-110	11.000	10.540	601	3.8	406
12	DW10 01	PCEA	10.000	9.566	610	3.9	406
11	BW1 03	NBG-18	9.000	8.591	619	4.1	406
10	FW01 03	IG-430	8.000	7.615	630	4.2	406
9	1H	Flux Monitor	7.375	7.003	636	4.3	406
8	CW1 02	H-451	6.750	6.395	643	4.3	406
7	EW02 01	IG-110	5.750	5.424	653	4.4	406
6	DW10 02	PCEA	4.750	4.454	662	4.5	406
5	BW10 01	NBG-18	3.750	3.482	669	4.5	406
4	FW01 04	IG-430	2.750	2.506	674	4.6	406
3	8H	Flux Monitor	2.125	1.895	676	4.6	406
2	AW1 01	NBG-17	1.500	1.286	677	4.6	406

Table B-2. Stack 1 uncompressed.

Loading Order	Specimen ID	Graphite Grade	Nominal Specimen Elevation (in)	End of Test Specimen Elevation (in)	Specimen Temperature (°C)	Specimen Dose (DPA)	Stack Load (lbf)
36	AW1 02	NBG-17	-1.750	-1.530	668	4.6	0
35	AO	Flux Monitor	-2.375	-2.153	664	4.6	0
34	FW02 01	IG-430	-3.000	-2.778	659	4.6	0
33	BW10 02	NBG-18	-4.000	-3.777	651	4.6	0
32	DW10 03	PCEA	-5.000	-4.775	642	4.5	0
31	EW02 02	IG-110	-6.000	-5.772	633	4.5	0
30	CW1 03	H-451	-7.000	-6.769	625	4.4	0
29	AL14 02	NBG-17	-7.625	-7.391	621	4.4	0
28	FW02 02	IG-430	-8.250	-8.015	616	4.3	0
27	BW10 03	NBG-18	-9.250	-9.014	610	4.2	0
26	DW10 04	PCEA	-10.250	-10.011	605	4.1	0
25	EW02 03	IG-110	-11.250	-11.009	601	4.0	0
24	FW02 03	IG-430	-12.250	-12.007	598	3.9	0
23	BW11 01	NBG-18	-13.250	-13.006	595	3.7	0
22	8U	Flux Monitor	-13.875	-13.631	593	3.6	0
21	DW11 01	PCEA	-14.500	-14.255	591	3.5	0
20	FW02 04	IG-430	-15.500	-15.254	587	3.3	0
19	EW02 04	IG-110	-16.500	-16.253	582	3.1	0
18	BW11 02	NBG-18	-17.500	-17.252	576	2.9	0
17	DW11 02	PCEA	-18.500	-18.251	568	2.7	0
16	AE	Flux Monitor	-19.125	-18.876	561	2.6	0
15	CW10 02	H-451	-19.750	-19.501	552	2.4	0
14	BP7 06	NBG-18	-20.375	-20.125	542	2.2	0
13	L2 08	PPEA	-20.625	-20.375	537	2.2	0
12	K2 09	PGX	-20.875	-20.624	532	2.1	0
11	P2-08	PCIB	-21.125	-20.874	526	2.0	0
10	DW18 03	PCEA	-21.375	-21.123	519	2.0	0
9	M2-07	NBG-25	-21.625	-21.373	512	1.9	0
8	S2 07	NBG-10	-21.875	-21.623	504	1.8	0
7	FW15 01	IG-430	-22.125	-21.873	496	1.8	0
6	EW14 01	IG-110	-22.375	-22.122	486	1.7	0
5	J2 06	HLM	-22.625	-22.372	476	1.6	0
4	RW2 09	BAN	-22.875	-22.622	464	1.6	0
3	H562	A3-3	-23.125	-22.871	451	1.5	0
2	TP 18	2114	-23.375	-23.120	437	1.4	0

Table B-3. Stack 2 compressed.

Loading Order	Specimen ID	Graphite Grade	Nominal Specimen Elevation (in)	End of Test Specimen Elevation (in)	Specimen Temperature (°C)	Specimen Dose (DPA)	Stack Load (lbf)
23	EW03 01	IG-110	19.500	18.656	542	2.0	508
22	AW17 07	NBG-17	18.875	18.045	550	2.2	508
21	FW03 01	IG-430	18.250	17.434	557	2.3	508
20	DA4 02	PCEA	17.250	16.461	567	2.6	508
19	BP4 02	NBG-18	16.250	15.489	574	2.8	508
18	AW1 03	NBG-17	15.250	14.515	579	3.0	508
17	EW03 02	IG-110	14.250	13.544	583	3.2	508
16	2B	Flux Monitor	13.625	12.937	586	3.4	508
15	DW11 03	PCEA	13.000	12.331	589	3.5	508
14	BW11 03	NBG-18	12.000	11.362	595	3.7	508
13	CW10 03	H-451	11.000	10.394	602	3.8	508
12	AW10 01	NBG-17	10.000	9.428	610	4.0	508
11	EW03 03	IG-110	9.000	8.462	620	4.1	508
10	DA4 03	PCEA	8.000	7.499	630	4.2	508
9	AW17 08	NBG-17	7.375	6.896	637	4.3	508
8	BP4 03	NBG-18	6.750	6.290	643	4.3	508
7	FW03 02	IG-430	5.750	5.323	653	4.4	508
6	AP4 02	NBG-17	4.750	4.355	661	4.5	508
5	CW11 01	H-451	3.750	3.391	668	4.6	508
4	DW11 04	PCEA	2.750	2.432	673	4.6	508
3	37	Flux Monitor	2.125	1.830	675	4.6	508
2	BW12 01	NBG-18	1.500	1.225	675	4.6	508

Table B-4. Stack 2 uncompressed.

Loading Order	Specimen ID	Graphite Grade	Nominal Specimen Elevation (in)	End of Test Specimen Elevation (in)	Specimen Temperature (°C)	Specimen Dose (DPA)	Stack Load (lbf)
36	BW12 02	NBG-18	-1.750	-1.612	666	4.7	0
35	AW17 09	NBG-17	-2.375	-2.232	662	4.7	0
34	DW12 01	PCEA	-3.000	-2.851	658	4.6	0
33	CW11 02	H-451	-4.000	-3.842	649	4.6	0
32	AP4 03	NBG-17	-5.000	-4.835	641	4.6	0
31	FW03 03	IG-430	-6.000	-5.830	632	4.5	0
30	BP5 01	NBG-18	-7.000	-6.825	624	4.4	0
29	EW15 09	IG-110	-7.625	-7.446	619	4.4	0
28	DA5 01	PCEA	-8.250	-8.067	615	4.3	0
27	EW03 04	IG-110	-9.250	-9.060	609	4.3	0
26	AW10 02	NBG-17	-10.250	-10.054	603	4.1	0
25	CW11 03	H-451	-11.250	-11.047	599	4.0	0
24	BW12 03	NBG-18	-12.250	-12.041	596	3.9	0
23	DW12 02	PCEA	-13.250	-13.035	593	3.7	0
22	7D	Flux Monitor	-13.875	-13.656	591	3.6	0
21	EW04 01	IG-110	-14.500	-14.278	589	3.5	0
20	AW10 03	NBG-17	-15.500	-15.274	585	3.3	0
19	BP5 02	NBG-18	-16.500	-16.270	581	3.1	0
18	DA5 02	PCEA	-17.500	-17.267	575	2.9	0
17	FW03 04	IG-430	-18.500	-18.264	567	2.7	0
16	EW15 10	IG-110	-19.125	-18.888	560	2.6	0
15	EW04 02	IG-110	-19.750	-19.511	552	2.4	0
14	J2 07	HLM	-20.375	-20.134	542	2.2	0
13	RW2 10	BAN	-20.625	-20.383	537	2.2	0
12	H571	A3-3	-20.875	-20.631	532	2.1	0
11	TP 19	2114	-21.125	-20.879	526	2.0	0
10	BP7 07	NBG-18	-21.375	-21.128	519	2.0	0
9	L2 09	PPEA	-21.625	-21.377	512	1.9	0
8	K2 10	PGX	-21.875	-21.626	504	1.8	0
7	P2-09	PCIB	-22.125	-21.875	496	1.8	0
6	DW18 04	PCEA	-22.375	-22.124	486	1.7	0
5	M2-08	NBG-25	-22.625	-22.374	476	1.6	0
4	S2 08	NBG-10	-22.875	-22.623	464	1.6	0
3	FW15 02	IG-430	-23.125	-22.872	451	1.5	0
2	EW14 02	IG-110	-23.375	-23.122	437	1.4	0

Table B-5. Stack 3 compressed.

Loading Order	Specimen ID	Graphite Grade	Nominal Specimen Elevation (in)	End of Test Specimen Elevation (in)	Specimen Temperature (°C)	Specimen Dose (DPA)	Stack Load (lbf)
23	CW12 02	H-451	19.500	18.614	542	2.0	606
22	TP 27	2114	18.875	18.004	550	2.2	606
21	DW12 03	PCEA	18.250	17.396	557	2.3	606
20	BW13 01	NBG-18	17.250	16.425	567	2.6	606
19	EW04 03	IG-110	16.250	15.454	574	2.8	606
18	FW04 01	IG-430	15.250	14.485	579	3.0	606
17	DW12 04	PCEA	14.250	13.518	584	3.2	606
16	2U	Flux Monitor	13.625	12.913	587	3.3	606
15	BW13 02	NBG-18	13.000	12.306	590	3.4	606
14	FW04 02	IG-430	12.000	11.338	597	3.6	606
13	EW04 04	IG-110	11.000	10.373	604	3.8	606
12	DW13 01	PCEA	10.000	9.413	613	3.9	606
11	BW13 03	NBG-18	9.000	8.451	622	4.0	606
10	FW04 04	IG-430	8.000	7.487	632	4.1	606
9	TP 12	2114	7.375	6.882	639	4.2	606
8	CW12 03	H-451	6.750	6.281	645	4.3	606
7	EW05 01	IG-110	5.750	5.323	654	4.3	606
6	DW13 02	PCEA	4.750	4.367	662	4.4	606
5	BW14 01	NBG-18	3.750	3.409	669	4.5	606
4	FW05 01	IG-430	2.750	2.446	673	4.5	606
3	8Y	Flux Monitor	2.125	1.843	675	4.5	606
2	AW11 01	NBG-17	1.500	1.241	675	4.6	606

Table B-6. Stack 3 uncompressed.

Loading Order	Specimen ID	Graphite Grade	Nominal Specimen Elevation (in)	End of Test Specimen Elevation (in)	Specimen Temperature (°C)	Specimen Dose (DPA)	Stack Load (lbf)
36	AW11 02	NBG-17	-1.750	-1.606	666	4.6	0
35	TP 24	2114	-2.375	-2.226	662	4.6	0
34	FW05 02	IG-430	-3.000	-2.849	657	4.6	0
33	BW14 02	NBG-18	-4.000	-3.844	649	4.5	0
32	DW13 03	PCEA	-5.000	-4.836	641	4.5	0
31	EW05 02	IG-110	-6.000	-5.828	632	4.4	0
30	CW13 01	H-451	-7.000	-6.820	624	4.4	0
29	TP 25	2114	-7.625	-7.440	619	4.3	0
28	FW05 03	IG-430	-8.250	-8.061	614	4.3	0
27	BW14 03	NBG-18	-9.250	-9.056	608	4.2	0
26	DW13 04	PCEA	-10.250	-10.050	603	4.1	0
25	EW05 03	IG-110	-11.250	-11.043	598	3.9	0
24	FW05 04	IG-430	-12.250	-12.038	595	3.8	0
23	BW15 01	NBG-18	-13.250	-13.034	591	3.7	0
22	1Y	Flux Monitor	-13.875	-13.656	590	3.6	0
21	DW14 01	PCEA	-14.500	-14.278	588	3.5	0
20	FW06 01	IG-430	-15.500	-15.274	584	3.3	0
19	EW05 04	IG-110	-16.500	-16.270	580	3.1	0
18	BW15 02	NBG-18	-17.500	-17.267	575	2.9	0
17	DW14 02	PCEA	-18.500	-18.264	567	2.7	0
16	TP 26	2114	-19.125	-18.887	560	2.5	0
15	CW13 02	H-451	-19.750	-19.511	552	2.4	0
14	DW18 05	PCEA	-20.375	-20.134	542	2.2	0
13	M2-09	NBG-25	-20.625	-20.383	537	2.1	0
12	S2 09	NBG-10	-20.875	-20.632	532	2.1	0
11	FW15 03	IG-430	-21.125	-20.881	526	2.0	0
10	EW14 03	IG-110	-21.375	-21.131	519	2.0	0
9	J2 08	HLM	-21.625	-21.380	512	1.9	0
8	RW4 01	BAN	-21.875	-21.629	504	1.8	0
7	H572	A3-3	-22.125	-21.878	496	1.7	0
6	TP 20	2114	-22.375	-22.126	486	1.7	0
5	L3 04	PPEA	-22.625	-22.375	476	1.6	0
4	L2 10	PPEA	-22.875	-22.625	464	1.5	0
3	K3 01	PGX	-23.125	-22.874	451	1.5	0
2	P2-10	PCIB	-23.375	-23.122	437	1.4	0

Table B-7. Stack 4 compressed.

Loading Order	Specimen ID	Graphite Grade	Nominal Specimen Elevation (in)	End of Test Specimen Elevation (in)	Specimen Temperature (°C)	Specimen Dose (DPA)	Stack Load (lbf)
23	EW06 01	IG-110	19.500	18.799	541	2.0	395
22	AX	Flux Monitor	18.875	18.185	549	2.1	395
21	FW06 02	IG-430	18.250	17.571	556	2.3	395
20	DA5 03	PCEA	17.250	16.590	566	2.5	395
19	BP5 03	NBG-18	16.250	15.609	573	2.7	395
18	AW11 03	NBG-17	15.250	14.629	579	2.9	395
17	EW06 02	IG-110	14.250	13.651	584	3.1	395
16	18	Flux Monitor	13.625	13.039	587	3.3	395
15	DW14 03	PCEA	13.000	12.429	591	3.4	395
14	BW15 03	NBG-18	12.000	11.452	597	3.5	395
13	CW13 03	H-451	11.000	10.476	604	3.7	395
12	AW12 01	NBG-17	10.000	9.502	613	3.8	395
11	EW06 03	IG-110	9.000	8.528	623	3.9	395
10	DA6 01	PCEA	8.000	7.557	633	4.1	395
9	AR	Flux Monitor	7.375	6.949	639	4.1	395
8	BP6 01	NBG-18	6.750	6.340	646	4.2	395
7	FW06 03	IG-430	5.750	5.365	655	4.3	395
6	AP5 01	NBG-17	4.750	4.390	664	4.3	395
5	CW2 01	H-451	3.750	3.419	670	4.4	395
4	DW14 04	PCEA	2.750	2.450	675	4.4	395
3	3F	Flux Monitor	2.125	1.843	676	4.4	395
2	BW16 01	NBG-18	1.500	1.233	677	4.5	395

Table B-8. Stack 4 uncompressed.

Loading Order	Specimen ID	Graphite Grade	Nominal Specimen Elevation (in)	End of Test Specimen Elevation (in)	Specimen Temperature (°C)	Specimen Dose (DPA)	Stack Load (lbf)
36	BW16 02	NBG-18	-1.750	-1.603	667	4.5	0
35	5B	Flux Monitor	-2.375	-2.224	663	4.5	0
34	DW15 02	PCEA	-3.000	-2.844	658	4.5	0
33	CW2 02	H-451	-4.000	-3.836	650	4.4	0
32	AP5 02	NBG-17	-5.000	-4.830	641	4.4	0
31	FW06 04	IG-430	-6.000	-5.825	632	4.3	0
30	BP6 02	NBG-18	-7.000	-6.820	624	4.3	0
29	AL14 03	NBG-17	-7.625	-7.441	619	4.2	0
28	DA6 02	PCEA	-8.250	-8.061	614	4.2	0
27	EW06 04	IG-110	-9.250	-9.055	608	4.1	0
26	AW12 02	NBG-17	-10.250	-10.049	602	4.0	0
25	CW2 03	H-451	-11.250	-11.043	598	3.9	0
24	BW16 03	NBG-18	-12.250	-12.038	594	3.7	0
23	DW15 03	PCEA	-13.250	-13.033	591	3.6	0
22	2Y	Flux Monitor	-13.875	-13.655	589	3.5	0
21	EW07 01	IG-110	-14.500	-14.277	588	3.4	0
20	AW12 03	NBG-17	-15.500	-15.272	584	3.2	0
19	BP6 03	NBG-18	-16.500	-16.269	580	3.0	0
18	DA7 01	PCEA	-17.500	-17.266	575	2.8	0
17	FW07 01	IG-430	-18.500	-18.264	567	2.6	0
16	8Z	Flux Monitor	-19.125	-18.888	560	2.5	0
15	EW07 02	IG-110	-19.750	-19.512	552	2.3	0
14	L3 05	PPEA	-20.375	-20.135	542	2.2	0
13	L3 01	PPEA	-20.625	-20.384	537	2.1	0
12	K3 02	PGX	-20.875	-20.633	532	2.0	0
11	P3-01	PCIB	-21.125	-20.882	526	2.0	0
10	DW18 06	PCEA	-21.375	-21.132	519	1.9	0
9	M2-10	NBG-25	-21.625	-21.381	512	1.9	0
8	S2 10	NBG-10	-21.875	-21.630	504	1.8	0
7	P3-06	PCIB	-22.125	-21.879	495	1.7	0
6	K3 05	PGX	-22.375	-22.128	486	1.7	0
5	J2 09	HLM	-22.625	-22.377	475	1.6	0
4	RW4 02	BAN	-22.875	-22.626	464	1.5	0
3	H581	A3-3	-23.125	-22.874	451	1.5	0
2	TP 21	2114	-23.375	-23.122	437	1.4	0

Table B-9. Stack 5 compressed.

Loading Order	Specimen ID	Graphite Grade	Nominal Specimen Elevation (in)	End of Test Specimen Elevation (in)	Specimen Temperature (°C)	Specimen Dose (DPA)	Stack Load (lbf)
23	CW3 01	H-451	19.500	18.545	543	2.0	503
22	EW15 11	IG-110	18.875	17.936	551	2.2	503
21	DW15 04	PCEA	18.250	17.328	558	2.3	503
20	BW2 01	NBG-18	17.250	16.355	567	2.6	503
19	EW07 03	IG-110	16.250	15.385	574	2.8	503
18	FW07 03	IG-430	15.250	14.415	580	3.0	503
17	DW16 01	PCEA	14.250	13.448	585	3.2	503
16	57	Flux Monitor	13.625	12.842	588	3.3	503
15	BW2 02	NBG-18	13.000	12.236	591	3.5	503
14	FW07 04	IG-430	12.000	11.268	597	3.6	503
13	EW07 04	IG-110	11.000	10.303	605	3.8	503
12	DW16 02	PCEA	10.000	9.342	614	3.9	503
11	BW2 03	NBG-18	9.000	8.378	624	4.1	503
10	FW08 01	IG-430	8.000	7.412	634	4.2	503
9	AW17 10	NBG-17	7.375	6.807	641	4.2	503
8	CW3 02	H-451	6.750	6.206	647	4.3	503
7	EW08 01	IG-110	5.750	5.247	657	4.4	503
6	DW16 03	PCEA	4.750	4.289	666	4.4	503
5	BW3 01	NBG-18	3.750	3.329	673	4.5	503
4	FW08 02	IG-430	2.750	2.365	677	4.5	503
3	AL	Flux Monitor	2.125	1.761	679	4.6	503
2	AW13 01	NBG-17	1.500	1.159	680	4.6	503

Table B-10. Stack 5 uncompressed.

Loading Order	Specimen ID	Graphite Grade	Nominal Specimen Elevation (in)	End of Test Specimen Elevation (in)	Specimen Temperature (°C)	Specimen Dose (DPA)	Stack Load (lbf)
36	AW13 02	NBG-17	-1.750	-1.592	671	4.6	0
35	EW15 08	IG-110	-2.375	-2.213	667	4.6	0
34	FW08 03	IG-430	-3.000	-2.836	662	4.6	0
33	BW3 02	NBG-18	-4.000	-3.832	653	4.5	0
32	DW16 04	PCEA	-5.000	-4.825	644	4.5	0
31	EW08 02	IG-110	-6.000	-5.818	635	4.4	0
30	CW3 03	H-451	-7.000	-6.811	626	4.4	0
29	EW15 07	IG-110	-7.625	-7.432	621	4.3	0
28	FW08 04	IG-430	-8.250	-8.055	617	4.3	0
27	BW3 03	NBG-18	-9.250	-9.050	610	4.2	0
26	DW17 01	PCEA	-10.250	-10.045	604	4.1	0
25	EW08 03	IG-110	-11.250	-11.039	599	4.0	0
24	FW09 01	IG-430	-12.250	-12.035	596	3.8	0
23	BW4 01	NBG-18	-13.250	-13.031	593	3.7	0
22	7Z	Flux Monitor	-13.875	-13.654	591	3.6	0
21	DW17 02	PCEA	-14.500	-14.277	589	3.5	0
20	FW09 02	IG-430	-15.500	-15.274	585	3.3	0
19	EW08 04	IG-110	-16.500	-16.270	581	3.1	0
18	BW4 02	NBG-18	-17.500	-17.267	575	2.9	0
17	DW17 04	PCEA	-18.500	-18.265	567	2.7	0
16	EW15 06	IG-110	-19.125	-18.888	561	2.5	0
15	CW4 01	H-451	-19.750	-19.512	552	2.4	0
14	J2 10	HLM	-20.375	-20.135	542	2.2	0
13	RW4 03	BAN	-20.625	-20.384	537	2.2	0
12	H582	A3-3	-20.875	-20.631	532	2.1	0
11	TP 22	2114	-21.125	-20.880	526	2.0	0
10	L3 06	PPEA	-21.375	-21.129	519	2.0	0
9	L3 02	PPEA	-21.625	-21.378	512	1.9	0
8	K3 03	PGX	-21.875	-21.627	504	1.8	0
7	P3-02	PCIB	-22.125	-21.876	496	1.8	0
6	DW18 07	PCEA	-22.375	-22.125	486	1.7	0
5	M2-11	NBG-25	-22.625	-22.374	476	1.6	0
4	S2 11	NBG-10	-22.875	-22.624	464	1.5	0
3	P3-05	PCIB	-23.125	-22.873	451	1.5	0
2	EW14 05	IG-110	-23.375	-23.122	437	1.4	0

Table B-11. Stack 6 compressed.

Loading Order	Specimen ID	Graphite Grade	Nominal Specimen Elevation (in)	End of Test Specimen Elevation (in)	Specimen Temperature (°C)	Specimen Dose (DPA)	Stack Load (lbf)
23	EW09 01	IG-110	19.500	18.608	543	2.1	604
22	TP 16	2114	18.875	17.999	551	2.2	604
21	FW09 03	IG-430	18.250	17.390	558	2.4	604
20	DA3 03	PCEA	17.250	16.418	567	2.6	604
19	BP4 01	NBG-18	16.250	15.446	575	2.8	604
18	AW13 03	NBG-17	15.250	14.474	580	3.0	604
17	EW09 02	IG-110	14.250	13.507	585	3.3	604
16	5F	Flux Monitor	13.625	12.902	588	3.4	604
15	DW2 01	PCEA	13.000	12.298	591	3.5	604
14	BW4 03	NBG-18	12.000	11.332	597	3.7	604
13	CW4 02	H-451	11.000	10.368	604	3.8	604
12	AW14 01	NBG-17	10.000	9.405	613	4.0	604
11	EA9 02	IG-110	9.000	8.443	623	4.1	604
10	DA3 02	PCEA	8.000	7.486	634	4.2	604
9	TP 17	2114	7.375	6.887	640	4.3	604
8	BP3 03	NBG-18	6.750	6.283	647	4.3	604
7	FW09 04	IG-430	5.750	5.320	657	4.4	604
6	AP5 03	NBG-17	4.750	4.357	666	4.5	604
5	CW4 03	H-451	3.750	3.397	673	4.6	604
4	DW2 02	PCEA	2.750	2.442	678	4.6	604
3	5H	Flux Monitor	2.125	1.844	680	4.6	604
2	BW5 01	NBG-18	1.500	1.241	681	4.6	604

Table B-12. Stack 6 uncompressed.

Loading Order	Specimen ID	Graphite Grade	Nominal Specimen Elevation (in)	End of Test Specimen Elevation (in)	Specimen Temperature (°C)	Specimen Dose (DPA)	Stack Load (lbf)
36	BW5 02	NBG-18	-1.750	-1.598	672	4.7	0
35	TP 13	2114	-2.375	-2.220	668	4.7	0
34	DW2 03	PCEA	-3.000	-2.840	663	4.6	0
33	CW5 01	H-451	-4.000	-3.832	655	4.6	0
32	AP6 01	NBG-17	-5.000	-4.826	646	4.6	0
31	FW10 01	IG-430	-6.000	-5.823	637	4.5	0
30	BP3 02	NBG-18	-7.000	-6.819	628	4.4	0
29	TP 14	2114	-7.625	-7.440	623	4.4	0
28	DA2 03	PCEA	-8.250	-8.061	619	4.3	0
27	EW09 04	IG-110	-9.250	-9.055	612	4.3	0
26	AW14 02	NBG-17	-10.250	-10.050	607	4.1	0
25	CW5 03	H-451	-11.250	-11.043	603	4.0	0
24	BW5 03	NBG-18	-12.250	-12.037	599	3.9	0
23	DW2 04	PCEA	-13.250	-13.032	596	3.7	0
22	7Y	Flux Monitor	-13.875	-13.653	594	3.6	0
21	EW10 01	IG-110	-14.500	-14.275	591	3.5	0
20	AW14 03	NBG-17	-15.500	-15.270	588	3.4	0
19	BP3 01	NBG-18	-16.500	-16.267	583	3.2	0
18	DA2 02	PCEA	-17.500	-17.263	577	2.9	0
17	FW10 02	IG-430	-18.500	-18.261	568	2.7	0
16	TP 15	2114	-19.125	-18.885	561	2.6	0
15	EW10 02	IG-110	-19.750	-19.509	553	2.4	0
14	CW14 06	H-451	-20.375	-20.132	542	2.2	0
13	M2-12	NBG-25	-20.625	-20.381	537	2.2	0
12	S2 12	NBG-10	-20.875	-20.630	532	2.1	0
11	K3 06	PGX	-21.125	-20.879	526	2.0	0
10	EW14 06	IG-110	-21.375	-21.129	519	2.0	0
9	J2 11	HLM	-21.625	-21.378	512	1.9	0
8	RW4 04	BAN	-21.875	-21.627	504	1.8	0
7	H591	A3-3	-22.125	-21.876	496	1.8	0
6	TP 23	2114	-22.375	-22.124	486	1.7	0
5	P3-04	PCIB	-22.625	-22.373	476	1.6	0
4	L3 03	PPEA	-22.875	-22.623	464	1.6	0
3	K3 04	PGX	-23.125	-22.873	451	1.5	0
2	P3-03	PCIB	-23.375	-23.122	437	1.4	0

Table B-13. Stack 7 uncompressed (1 of 6).

Loading Order	Specimen ID	Graphite Grade	Nominal Specimen Elevation (in)	End of Test Specimen Elevation (in)	Specimen Temperature (°C)	Specimen Dose (DPA)
170	A3-P43-Z12	A3-27	18.375	18.383	624	2.2
169	J1 11	HLM	18.125	18.134	614	2.3
168	K2 02	PGX	17.875	17.886	607	2.3
167	L2 01	PPEA	17.625	17.637	601	2.4
166	M1-12	NBG-25	17.375	17.388	597	2.4
165	TP 11	2114	17.125	17.139	593	2.5
164	P2-01	PCIB	16.875	16.890	591	2.6
163	RW2 02	BAN	16.625	16.641	590	2.6
162	S1 11	NBG-10	16.375	16.392	589	2.7
161	CPB101	HOPG CAN	16.125	16.143	590	2.7
160	BP7 08	NBG-18	15.875	15.894	590	2.8
159	DW18 08	PCEA	15.625	15.645	591	2.8
158	BP7 09	NBG-18	15.375	15.396	592	2.9
157	FW15 04	IG-430	15.125	15.147	594	3.0
156	EW14 04	IG-110	14.875	14.898	596	3.0
155	CW14 05	H-451	14.625	14.649	598	3.1
154	A3-H08-Z19	A3-27	14.375	14.401	600	3.1
153	J1 10	HLM	14.125	14.154	602	3.2
152	K2 01	PGX	13.875	13.905	604	3.2
151	L1 10	PPEA	13.625	13.657	606	3.3
150	M1-11	NBG-25	13.375	13.408	609	3.3
149	TP 10	2114	13.125	13.160	611	3.4
148	P1-10	PCIB	12.875	12.910	613	3.4
147	RW2 01	BAN	12.625	12.661	615	3.5
146	S1 10	NBG-10	12.375	12.412	618	3.5
145	CPB91	HOPG CAN	12.125	12.164	620	3.5
144	BP7 10	NBG-18	11.875	11.915	622	3.6
143	DA8 05	PCEA	11.625	11.667	624	3.6
142	AP7 08	NBG-17	11.375	11.418	627	3.7
141	FW15 05	IG-430	11.125	11.169	629	3.7

Table B-14. Stack 7 uncompressed (2 of 6).

Loading Order	Specimen ID	Graphite Grade	Nominal Specimen Elevation (in)	End of Test Specimen Elevation (in)	Specimen Temperature (°C)	Specimen Dose (DPA)
140	EW15 03	IG-110	10.875	10.920	631	3.7
139	CW14 04	H-451	10.625	10.672	634	3.8
138	H521	A3-3	10.375	10.424	636	3.8
137	J1 09	HLM	10.125	10.176	638	3.9
136	K1 10	PGX	9.875	9.928	641	3.9
135	L1 09	PPEA	9.625	9.680	643	3.9
134	M1-10	NBG-25	9.375	9.432	645	4.0
133	TP 09	2114	9.125	9.184	648	4.0
132	P1-09	PCIB	8.875	8.935	650	4.0
131	RW1 10	BAN	8.625	8.686	653	4.1
130	S1 09	NBG-10	8.375	8.438	655	4.1
129	CPB81	HOPG CAN	8.125	8.190	658	4.1
128	BW17 01	NBG-18	7.875	7.941	660	4.2
127	DA8 04	PCEA	7.625	7.693	663	4.2
126	AP7 09	NBG-17	7.375	7.444	665	4.2
125	FW15 06	IG-430	7.125	7.196	668	4.2
124	EW15 02	IG-110	6.875	6.947	670	4.3
123	CW14 03	H-451	6.625	6.698	673	4.3
122	H512	A3-3	6.375	6.449	675	4.3
121	J1 08	HLM	6.125	6.201	677	4.3
120	K1 09	PGX	5.875	5.953	680	4.3
119	L1 08	PPEA	5.625	5.704	682	4.4
118	M1-09	NBG-25	5.375	5.456	684	4.4
117	TP 08	2114	5.125	5.207	687	4.4
116	P1-08	PCIB	4.875	4.958	689	4.4
115	RW1 09	BAN	4.625	4.709	691	4.4
114	S1 08	NBG-10	4.375	4.461	693	4.5
113	CPB71	HOPG CAN	4.125	4.212	695	4.5
112	BW17 09	NBG-18	3.875	3.964	696	4.5
111	DA8 03	PCEA	3.625	3.715	698	4.5

Table B-15. Stack 7 uncompressed (3 of 6).

Loading Order	Specimen ID	Graphite Grade	Nominal Specimen Elevation (in)	End of Test Specimen Elevation (in)	Specimen Temperature (°C)	Specimen Dose (DPA)
110	AP7 10	NBG-17	3.375	3.467	700	4.5
109	FW16 01	IG-430	3.125	3.218	701	4.5
108	EW15 01	IG-110	2.875	2.969	702	4.5
107	CPB151	HOPG CAN	2.625	2.720	703	4.6
106	A3-P33-Z09	A3-27	2.375	2.469	704	4.6
105	J1 07	HLM	2.125	2.218	705	4.6
104	K1 08	PGX	1.875	1.971	706	4.6
103	L1 07	PPEA	1.625	1.723	707	4.6
102	M1-08	NBG-25	1.375	1.474	707	4.6
101	TP 07	2114	1.125	1.226	707	4.6
100	P1-07	PCIB	0.875	0.977	707	4.6
99	RW1 08	BAN	0.625	0.728	707	4.6
98	S1 07	NBG-10	0.375	0.479	707	4.6
97	CPB61	HOPG CAN	0.125	0.231	707	4.6
96	BW17 08	NBG-18	-0.125	-0.017	706	4.6
95	DA8 02	PCEA	-0.375	-0.266	705	4.6
94	AW17 01	NBG-17	-0.625	-0.513	704	4.6
93	FW15 12	IG-430	-0.875	-0.761	703	4.6
92	EW14 12	IG-110	-1.125	-1.010	702	4.6
91	CPB141	HOPG CAN	-1.375	-1.259	701	4.6
90	A3-H08-Z07	A3-27	-1.625	-1.509	700	4.6
89	J1 06	HLM	-1.875	-1.759	698	4.6
88	K1 07	PGX	-2.125	-2.006	697	4.6
87	L1 06	PPEA	-2.375	-2.253	695	4.6
86	M1-07	NBG-25	-2.625	-2.501	693	4.6
85	TP 06	2114	-2.875	-2.750	691	4.6
84	P1-06	PCIB	-3.125	-2.998	689	4.6
83	RW1 07	BAN	-3.375	-3.246	687	4.6
82	S1 06	NBG-10	-3.625	-3.495	685	4.6
81	CPB51	HOPG CAN	-3.875	-3.743	683	4.6

Table B-16. Stack 7 uncompressed (4 of 6).

Loading Order	Specimen ID	Graphite Grade	Nominal Specimen Elevation (in)	End of Test Specimen Elevation (in)	Specimen Temperature (°C)	Specimen Dose (DPA)
80	BW17 07	NBG-18	-4.125	-3.991	681	4.6
79	DA8 01	PCEA	-4.375	-4.239	678	4.6
78	AW17 02	NBG-17	-4.625	-4.488	676	4.5
77	FW15 11	IG-430	-4.875	-4.736	674	4.5
76	EW14 11	IG-110	-5.125	-4.985	671	4.5
75	CPB131	HOPG CAN	-5.375	-5.233	669	4.5
74	A3-P43-Z03	A3-27	-5.625	-5.483	667	4.5
73	J1 05	HLM	-5.875	-5.731	664	4.5
72	K1 06	PGX	-6.125	-5.979	662	4.5
71	L1 05	PPEA	-6.375	-6.226	660	4.4
70	M1-06	NBG-25	-6.625	-6.474	658	4.4
69	TP 05	2114	-6.875	-6.722	655	4.4
68	P1-05	PCIB	-7.125	-6.970	653	4.4
67	RW1 06	BAN	-7.375	-7.218	651	4.4
66	S1 05	NBG-10	-7.625	-7.466	649	4.4
65	CPB41	HOPG CAN	-7.875	-7.714	647	4.3
64	BW17 05	NBG-18	-8.125	-7.963	645	4.3
63	DW18 12	PCEA	-8.375	-8.211	643	4.3
62	AW17 03	NBG-17	-8.625	-8.458	641	4.3
61	FW15 10	IG-430	-8.875	-8.706	640	4.2
60	EW14 10	IG-110	-9.125	-8.955	638	4.2
59	CPB121	HOPG CAN	-9.375	-9.204	636	4.2
58	H491	A3-3	-9.625	-9.453	635	4.2
57	J1 04	HLM	-9.875	-9.701	633	4.1
56	K1 05	PGX	-10.125	-9.948	632	4.1
55	L1 04	PPEA	-10.375	-10.195	630	4.1
54	M1-05	NBG-25	-10.625	-10.443	629	4.1
53	TP 04	2114	-10.875	-10.691	628	4.0
52	P1-04	PCIB	-11.125	-10.939	627	4.0
51	RW1 05	BAN	-11.375	-11.188	625	4.0

Table B-17. Stack 7 uncompressed (5 of 6).

Loading Order	Specimen ID	Graphite Grade	Nominal Specimen Elevation (in)	End of Test Specimen Elevation (in)	Specimen Temperature (°C)	Specimen Dose (DPA)
50	S1 04	NBG-10	-11.625	-11.435	624	3.9
49	CPB31	HOPG CAN	-11.875	-11.684	623	3.9
48	BW17 04	NBG-18	-12.125	-11.933	622	3.9
47	DW18 11	PCEA	-12.375	-12.181	621	3.8
46	AW17 06	NBG-17	-12.625	-12.429	620	3.8
45	FW15 09	IG-430	-12.875	-12.677	619	3.8
44	EW14 09	IG-110	-13.125	-12.926	618	3.7
43	CPB111	HOPG CAN	-13.375	-13.175	617	3.7
42	H482	A3-3	-13.625	-13.423	616	3.6
41	J1 03	HLM	-13.875	-13.671	615	3.6
40	K1 04	PGX	-14.125	-13.918	614	3.6
39	L1 03	PPEA	-14.375	-14.166	612	3.5
38	M1-04	NBG-25	-14.625	-14.414	611	3.5
37	TP 03	2114	-14.875	-14.663	610	3.4
36	P1-03	PCIB	-15.125	-14.911	609	3.4
35	RW1 04	BAN	-15.375	-15.160	607	3.3
34	S1 03	NBG-10	-15.625	-15.409	606	3.3
33	CPB21	HOPG CAN	-15.875	-15.658	605	3.2
32	BW17 03	NBG-18	-16.125	-15.907	603	3.2
31	DW18 10	PCEA	-16.375	-16.156	601	3.1
30	AW17 05	NBG-17	-16.625	-16.404	600	3.1
29	FW15 08	IG-430	-16.875	-16.653	598	3.0
28	EW14 08	IG-110	-17.125	-16.902	596	3.0
27	CA11 02	H-451	-17.375	-17.151	594	2.9
26	A3-P33-Z20	A3-27	-17.625	-17.400	592	2.9
25	J1 02	HLM	-17.875	-17.648	589	2.8
24	K1 03	PGX	-18.125	-17.896	587	2.8
23	L1 02	PPEA	-18.375	-18.144	584	2.7
22	M1-02	NBG-25	-18.625	-18.393	581	2.7
21	TP 02	2114	-18.875	-18.642	578	2.6

Table B-18. Stack 7 uncompressed (6 of 6).

Loading Order	Specimen ID	Graphite Grade	Nominal Specimen Elevation (in)	End of Test Specimen Elevation (in)	Specimen Temperature (°C)	Specimen Dose (DPA)
20	P1-02	PCIB	-19.125	-18.891	575	2.5
19	RW1 03	BAN	-19.375	-19.140	571	2.5
18	S1 02	NBG-10	-19.625	-19.390	567	2.4
17	CPB11	HOPG CAN	-19.875	-19.639	563	2.4
16	BW17 02	NBG-18	-20.125	-19.888	558	2.3
15	DW18 09	PCEA	-20.375	-20.137	553	2.2
14	AW17 04	NBG-17	-20.625	-20.387	548	2.2
13	FW15 07	IG-430	-20.875	-20.636	542	2.1
12	EW14 07	IG-110	-21.125	-20.885	535	2.0
11	CA11 01	H-451	-21.375	-21.135	528	2.0
10	H472	A3-3	-21.625	-21.383	520	1.9
9	J1 01	HLM	-21.875	-21.631	511	1.8
8	K1 01	PGX	-22.125	-21.880	501	1.8
7	L1 01	PPEA	-22.375	-22.128	490	1.7
6	M1-01	NBG-25	-22.625	-22.377	478	1.6
5	TP 01	2114	-22.875	-22.626	464	1.6
4	P1-01	PCIB	-23.125	-22.875	449	1.5
3	RW1 02	BAN	-23.375	-23.124	432	1.4
2	CPB1	HOPG CAN	-23.625	-23.374	413	1.3
1	S1 01	NBG-10	-23.875	-23.624	392	1.3